fermentation

MDPI

Article

In Silico Prediction of Secondary Metabolites and Biosynthetic Gene Clusters Analysis of *Streptomyces thinghirensis* HM3 Isolated from Arid Soil

Medhat Rehan [1,2,*], Abdellatif Gueddou [3], Abdulaziz Alharbi [1] and Imen Ben Abdelmalek [4]

[1] Department of Plant Production and Protection, College of Agriculture and Veterinary Medicine, Qassim University, Buraydah 51452, Saudi Arabia
[2] Department of Genetics, Faculty of Agriculture, Kafrelsheikh University, Kafr El-Sheikh 33516, Egypt
[3] Department of Molecular, Cellular and Biomedical Sciences, College of Life Sciences, University of New Hampshire, Durham, NH 03824, USA
[4] Department of Biology, College of Science, Qassim University, Buraydah 52571, Saudi Arabia
* Correspondence: m.rehan@qu.edu.sa or medhat.rehan@agr.kfs.edu.eg

Abstract: Natural products produced by microorganisms are considered an important resource of bioactive secondary metabolites, such as anticancer, antifungal, antibiotic, and immunosuppressive molecules. *Streptomyces* are the richest source of bioactive natural products via possessing a wide number of secondary metabolite biosynthetic gene clusters (SM-BGCs). Based on rapid development in sequencing technologies with advances in genome mining, exploring the newly isolated *Streptomyces* species for possible new secondary metabolites is mandatory to find novel natural products. The isolated *Streptomyces thinghirensis* strain HM3 from arid and sandy texture soil in Qassim, SA, exerted inhibition activity against tested animal pathogenic Gram-positive bacteria and pathogenic fungal species. In this study, we report the draft genome of *S. thinghirensis* strain HM3, which consists of 7,139,324 base pairs (bp), with an average G+C content of 71.49%, predicting 7949 open reading frames, 12 rRNA operons (5S, 16S, 23S) and 60 tRNAs. An in silico analysis of strain HM3 genome by the antiSMASH and PRISM 4 online software for SM-BGCs predicted 16 clusters, including four terpene, one lantipeptide, one siderophore, two polyketide synthase (PKS), two non-ribosomal peptide synthetase (NRPS) cluster)/NRPS-like fragment, two RiPP/RiPP-like (ribosomally synthesised and post-translationally modified peptide product), two butyrolactone, one CDPS (tRNA-dependent cyclodipeptide synthases), and one other (cluster containing a secondary metabolite-related protein that does not fit into any other category) BGC. The presented BGCs inside the genome, along with antibacterial and antifungal activity, indicate that HM3 may represent an invaluable source for new secondary metabolites.

Keywords: *Streptomyces*; arid soil; secondary metabolites; genome sequencing; data mining; BGCs

Citation: Rehan, M.; Gueddou, A.; Alharbi, A.; Ben Abdelmalek, I. In Silico Prediction of Secondary Metabolites and Biosynthetic Gene Clusters Analysis of *Streptomyces thinghirensis* HM3 Isolated from Arid Soil. *Fermentation* **2023**, *9*, 65. https://doi.org/10.3390/fermentation9010065

Academic Editors: Teresa Gervasi, Giuseppina Mandalari and Johannes Wöstemeyer

Received: 7 November 2022
Revised: 23 December 2022
Accepted: 9 January 2023
Published: 12 January 2023

1. Introduction

Streptomyces [1], the leading bacterial genus of the family *Streptomycetaceae*, have been the subject of investigations for over a century, particularly following the discovery of their prodigious ability to produce interesting secondary metabolites and bioactive compounds with important biological activities [2–6]. Strains belonging to the genus *Streptomyces*, members of the order Actinomycetales within the class Actinobacteria [7], are Gram-positive, aerobic, spore-forming, and possess a very high G+C content (69 ± 78 mol%.) with complex multicellular morphology [8]. *Streptomyces* species are widespread and able to colonize several aquatic and terrestrial ecosystems. The genus members are ubiquitous in the soil environment, where they grow as a substrate mycelium composed of multiple hyphae, but some strains are able to live in symbiosis with eukaryotic organisms, most notably plants, fungi, and animals [9].

Streptomyces strains have served as the major producer of bioactive natural products, medicinal chemicals, and novel drugs, contributing 62% of the microbe-derived antibiotics from the 1950s to the 1970s [10]. Yet, studies estimate that *Streptomyces* species can synthesize some 150,000 more antimicrobial compounds than those currently known, highlighting the genus as a significant resource of new innovations in secondary metabolites discovery [11–14]. *Streptomyces* produce clinically useful antibiotics and highly valuable pharmaceutical products, including anticancer, immunostimulatory, immunosuppressive, antioxidative agents, insecticides, and antiparasitic drugs, which have bio-economic benefits and broad medical and agricultural applications [15]. *Streptomyces* produce antibacterial, antifungal, and certain wide-spectrum antibiotics such as rifamycins, chloramphenicol, fungichromin, macrolides (erythromycin and its relatives), and aminoglycosides (streptomycin and its relatives), and are, thus, considered to be rich biotechnological cell factories [16–21]. They also produce broad-spectrum insecticides and antiparasitic bioactive agents with strong activity against arthropods and nematodes, such as Ivermectin [22]. *Streptomyces* spp. are a valuable source of active metabolites applied on several crops to control several phytopathogenic microorganisms, and they are used to promote plant growth through the siderophore or auxin production [23–25]. Numerous *Streptomyces* species exhibit a remarkable capacity for the production of industrially high economic value enzymes such as α-amylases, cellulases, alkaline protease, keratinases, lipases, uricase, cholesterol oxidase, and L-asparaginase [26]. Recently, the use of *Streptomyces* species as environmentally friendly "nanofactories" for nanoparticle biosynthesis has been suggested by many scientists [27,28].

Researchers around the world continue to explore the enormous potential of *Streptomyces* using the latest developed strategies of modification of culture conditions, bioinformatics and genome mining, genome editing tools, heterologous expression, and other approaches [3–29]. The integration of genome-scale DNA sequencing with various omics technologies is a helpful tool to select effective-production organisms, through the assessment of their metabolic capacities, and has provided more information regarding the biosynthetic pathways of secondary metabolites that will expand the biotechnological and industrial applications of *Streptomyces* species [30–32]. Based on the resistance of infectious diseases to drugs, looking for new drugs to break down this resistance is vital and urgent. Novel bioactive natural products from *Streptomyces* are eagerly anticipated including clinical and agricultural antibiotics, immunosuppressant agents, antitumour, antifungal and antibacterial drugs [33].

In this study, we aimed to evaluate the antibacterial and antifungal activities of *S. thinghirensis* strain HM3, a strain isolated from Qassim, Saudi Arabia, and to sequence its genome. The genome was subjected to comprehensive phylogenetic, genomic, and secondary metabolic analyses to search for a possible new source of natural products.

2. Materials and Methods

2.1. Soil Properties, Cultural Conditions, and Antimicrobial Assay

S. thinghirensis strain HM3 (Accession: MN527231) [34,35] was isolated from Qassim University campus, SA, with soil characteristics (Table 1), as follows:

Table 1. Soil properties of isolated strain *S. thinghirensis* strain HM3.

pH	EC	OM	C/N	N	P	K	Particle Size Analysis			Texture
	(dS m^{-1})	(%)	Ratio		mg kg^{-1}		Sand (%)	Silt (%)	Clay (%)	
7.90	3.2	0.25	35	42	4.6	35	98.0	1.2	0.8	Sand

- pH was measured in the soil aqueous extract (soil:water) at a ratio of (1:2.5) using a pH meter type (Jenway, model 3310), according to the method of Page et al. [36].

- EC (electrical conductivity, dS m^{-1}) was measured in the saturated soil paste extract and estimated using an EC-meter type (ELE, model 470), according to the method recommended in the study of Jackson [37].
- Total N was determined by the Kjeldahl method; P was extracted using the Olsen method; K by 1 N NH_4OAc at pH 7, Page et al. [36].
- Organic matter (OM, %) was determined in soil by the modified Walkley–Black method, according to Nelson and Sommers [38].
- Particle size analysis and soil texture were measured by Gee [39].

Tryptic Soy Agar/broth (TSA/B) composed of peptic digest of soybean meal (5.0 g/L), sodium chloride (5.0 g/L), agar (15.0 g/L), pH 7.5, was used for regular growth and maintenance. For spore production, glucose soybean meal agar (GSA), which consisted of (g/L), 10 soybean meal, 10 glucose, 1 $CaCO_3$, 10 NaCl, and pH adjusted to 7.0 with NaOH (0.5 N), was used to grow the HM3 strain for 5 days at 30 °C. PDA and Muller Hinton media were chosen for secondary metabolites production in antifungal and antibacterial assays, as previously described by Rehan et al. [34] and Qureshi et al. [40]. In antibacterial assay, eight animal pathogenic bacteria, four as a Gram-positive, *Streptococcus pneumoniae* ATCC 49619, *Staphylococcus aureus* ATCC 29213, Methicillin-resistant *Staphylococcus aureus* (MRSA-A), *Enterococcus faecalis* ATCC 29212, plus four Gram-negative bacteria *Pseudomonas aerugenosa* ATCC 9027, *Proteus mirabilis* ATCC 29906, *Escherichia coli* ATCC 25922, and *Klebsiella pneumoniae* ATCC 27736, were selected for this purpose. One single colony form *Streptomyces* grown on GSA medium was used to inoculate Muller Hinton agar medium spread with each of the animal pathogenic bacteria, and an inhibition zone was observed around the inoculated strains. Moreover, ten fungal strains were screened against the selected HM3 strain [34]. Briefly, a 6 mm disk from fungal mycelium was placed in the centre of a PDA plate and a single colony from *Streptomyces* placed into the opposite sides of each PDA plate, then incubated at 30 °C for five days.

2.2. Genomic DNA Extraction and Whole Genome Sequencing

To extract genomic DNA (gDNA) from *S. thinghirensis* strain HM3, a cetyltrimethylammonium bromide (CTAB) protocol was applied [41]. The bacterial culture was grown in Czapek broth medium for 5 days at 28 °C. The bacterial cells were collected from 5 mL of Czpeck liquid culture by centrifugation at 14,000× *g* for 5 min. The biomass was re-suspended in TE buffer (10 mM of Tris; 1 mM of EDTA, pH 8.0) and homogenized by successive passing through a 0.1 mm diameter sterile syringe needle. We added 20 µL of 100 mg/mL lysozyme (EM Science, Darmstadt, Germany) to the homogenized cells and incubated them at 37 °C to break down the cell walls. After 30 min, 8 µL of 20 mg/mL proteinase K was added and incubated overnight at 56 °C to digest the residual proteins. The gDNA was purified by phenol-chloroform extractions, cleaned, and concentrated by mixing with 1 volume AMPure beads (Beckman Coulter Life Sciences, Brea, CA, USA), according to the manufacturer's instructions. The dried DNA pellets were dissolved in 50 µL of Tris-HCl Buffer (10 mM with 50 mM of NaCl, pH 8.0), and the purity of the genomic DNA was checked using an Invitrogen Qubit® 3.0 fluorometer and the 1× Qubit double-stranded DNA (dsDNA) high-sensitivity (HS) assay kit (Thermo Fisher Scientific, Waltham, MA, USA), then stored at −20 °C.

DNA libraries were prepared for long-read sequencing using the ONT rapid barcoding genomic sequencing kit (SQK-RBK004; Oxford Nanopore Technologies, Inc., Oxford, UK) and loaded without size selection onto the primed MinIONSpotON flow cell (R9.4.1 FLO-MIN 106; ONT, Oxford, UK) according to the manufacturer's protocol. Genome sequencing was conducted by an Oxford Nanopore's MinIONMk1C device (ONT, Oxford, UK) connected to MinKNOW version 22.05.8 for 48 h real-time base calling in high-accuracy mode, with a quality score cut-off of 7.

2.3. Genome Assembly, Annotation, and Data Availability

For de novo assembly of the genome, all generated reads in FASTQ format that passed quality control were assembled using the EPI2ME Labs platform (Oxford Nanopore Technologies, Oxford, UK) employing the assembler Flye version 2.8.1-b1676 [42]. To obtain contigs with high accuracy, the assembled contigs were subject to a first-step assembly polishing with Racon (v1.4.16) [43], followed by a second polishing by the Medaka (v1.5.0) consensus program [44]. The statistics of the final polished consensus were calculated using QUAST v5.2.0 [45]. The completeness and contamination of the assembled genome were estimated by CheckM [46]. The generated genome assembly was annotated at NCBI with the Prokaryotic Genome Annotation Pipeline (PGAP) [47]. All software was run using default parameters.

The raw sequencing reads were deposited in the NCBI Sequence Read Archive (SRA) under the accession number SRR17278423. The *S. thinghirensis* strain HM3 genome sequence was deposited at NCBI GenBank under accession ID JAKFGP000000000 and BioProject accession number PRJNA790006.

2.4. Phylogenetic Analysis Based on 16S rRNA Gene and Whole Genome Sequencing

To achieve a true phylogenetic analysis based on the whole-genome and the 16S rRNA gene of *S. thinghirensis* strain HM3, the assembled FASTA contigs file was run through the Type (Strain) Genome Server (TYGS), a free bioinformatics platform available at https://tygs.dsmz.de/ (accessed on 20 July 2022) [48]. The genome was compared against all type strain genomes available in the TYGS database via the MASH algorithm [48,49]. TYGS provides the closest related type strains by using the Genome Blast Distance Phylogeny (GBDP) to calculate the digital DNA-DNA hybridization (dDDH) and the intergenomic distances to infer the phylogenetic trees [48]. The Average Nucleotide Identity (ANI) comparisons of the genomes were calculated using OrthoANI using USEARCH in the ChunLab webserver [50]. The 16S rRNA gene sequence of *S. thinghirensis* strain HM3 was extracted from the genome using RNAmmer [51], and BLAST [52] was used to perform an alignment against the 16S rRNA gene sequences of all type strains currently available in the TYGS database, as well as to infer the 16S phylogenetic tree. The 16S rRNA gene sequence was also manually extracted using barrnap 0.9 and used for the BLAST search in the NCBI database.

2.5. Metabolites Analysis and Identification of Putative Biosynthetic Gene Clusters (BGCs)

To identify the biosynthetic gene clusters (BGCs), *S. thinghirensis* strain HM3 genome was submitted to antiSMASH bacterial version (antiSMASH 6.0: improving cluster detection and comparison capabilities, accessed on 20 July 2022) [53] and PRISM (PRediction Informatics for Secondary Metabolomes) [54] to identify unknown secondary metabolite biosynthesis gene clusters and their predicted chemical structures. antiSMASH uses a hidden Markov models (HMMs) based probabilistic algorithm to detect BGC regions in genomes. PFAM: the protein families database [55], the Minimum Information about a Biosynthetic Gene cluster (MIBiG) [56], were used for further domain function, annotations and metadata on biosynthetic gene clusters and their molecular products. KnownClusterBlast and ClusterBlast modules were used to identify similar clusters in the selected genome by genome comparisons. Furthermore, non-ribosomal peptide synthetases/polyketide synthases (NRPSs/PKSs) modules were applied for cluster-specific analyses, which will provide more information and predictions about the biosynthetic compound.

3. Results

3.1. Antimicrobial Activity of S. thinghirensis Strain HM3

S. thinghirensis HM3 was isolated from alkaline sandy soil that was rich in carbon and poor in nitrogen (C/N = 35), phosphate, potassium, and organic matter. Based on soil electrical conductivity (EC), this soil was classified as normal or slightly saline. Preliminary antimicrobial screening of strain HM3 by the spot inoculation method revealed

inhibition activity with Gram-positive bacteria, including *S. pneumoniae* ATCC 49619, *S. aureus* ATCC 29213, and MRSA-A (Figure 1), whereas no activity was detected against the Gram-negative bacteria tested. On the other hand, the HM3 strain exerted inhibitory effects against ten pathogenic fungal species, i.e., *Thielaviopsis basicola, Colletotrichum gloeosporides, Botrytis cinerea, Myrothecium roridum, Rhizoctonia solani, Fusarium oxysporum, Fusarium graminearum, Alternaria solani, Fusarium solani,* and *Fusarium moniliforme*, as previously shown by Rehan et al. [34].

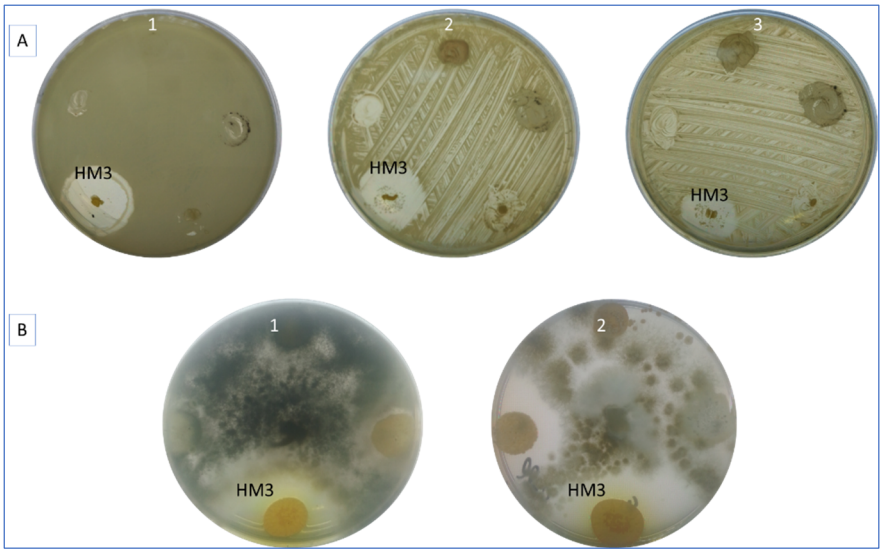

Figure 1. Antibacterial and antifungal activities of *S. thinghirensis* HM3 (**A**) against three animal pathogenic and Gram-positive bacteria; (1) S. pneumoniae ATCC 49619, (2) S. aureus ATCC 29213, (3) MRSA-A. (**B**) against soil-borne disease fungi; (1) Thielaviopsis basicola, (2) Colletotrichum gloeosporides.

3.2. Whole Genome Sequencing and General Genome Features

A total of 30,937 reads were generated by Nanopore sequencing and had a total read length of 44,764,953 sequenced bases. The average length of the reads was 1446.97 bp, with a maximum length of 116,217 bp and a N_{50} value of 10,193 bp.

As summarized in Table 2, the total length of the assembled draft genome was 7.14 Mbp (genome coverage of 6.27×), with an average GC content of 71.49%. The final assembly was composed of 69 contigs (N_{50}, 174,705 bp; L_{50}, 13), where the largest contig was 478,557 bp. The assembly contained 7949 gene sequence predictions, 3362 protein-coding sequences, 12 complete rRNA genes, and 60 tRNAs (Table 2).

Table 2. General genome features.

Statistics	***S. thinghirensis* Strain HM3**
contigs number	69
Largest contig (bp)	478,557
Total length (bp)	7,139,324
N_{50}	174,705
N_{75}	88,698
L_{50}	13
L_{75}	27
GC (%)	71.49
Genes (total)	7949
Coding genes	3362
Genes (RNA)	75
rRNAs	4, 4, 4 (5S, 16S, 23S)
tRNA	60
Pseudo genes (total)	4512

3.3. Phylogenetic Analysis and Genome Comparison with Other Streptomyces

The phylogenetic position of the S. thinghirensis strain HM3 was assessed using Type (Strain) Genome Server (https://tygs.dsmz.de/, accessed on 20 July 2022). A BLAST search with the 1523 bp 16S rRNA gene sequence of strain HM3 and a whole-genome sequence-based comparison (Figure S1) showed that HM3 displayed greater than 99% sequence similarity to the 16S rRNA gene and genome sequences of many species of the genus Streptomyces (Figure 2). The phylogenetic analysis showed that strain HM3 branched off separately from the other closest Streptomyces species group and was most closely related to Streptomyces ambofaciens ATCC 23877 (Figure 2). The BLAST results showed that the highest degree of similarity was found with Streptomyces ambofaciens ATCC 23877 (99.48%), Streptomyces albogriseolus (99.32%), Streptomyces griseorubens (99.32%), Streptomyces viridodiastaticus (99.32%), and Streptomyces thinghirensis (99.32%). The TYGS analysis identified 18 type strains that were most similar to the HM3 genome (Supplementary Material S1). All the identified type strains had a dDDH value less than 70% (32.1–49.2%; Supplementary Material S1). The genome sequence of HM3 showed an ANI less than 95% (88.57%) when compared to the clustered closer strain, Streptomyces ambofaciens ATCC 23877, thus confirming that it could represent a novel species within the genus Streptomyces.

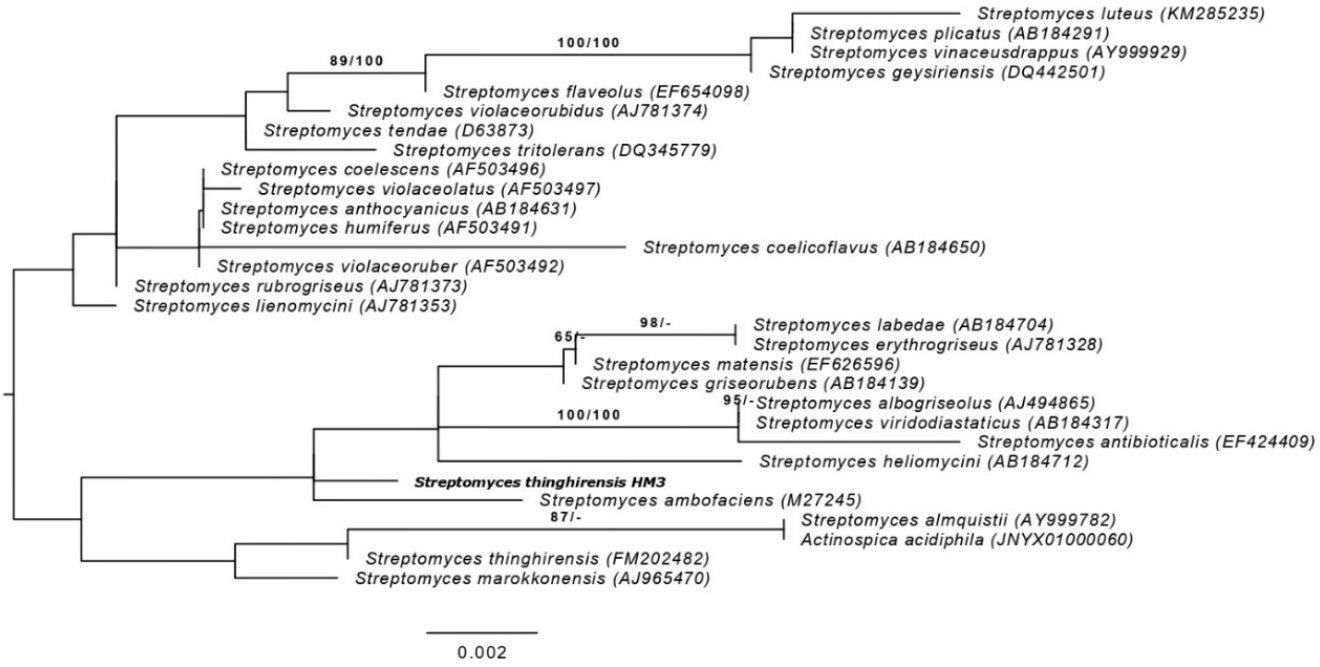

Figure 2. Phylogenetic tree inferred with FastME 2.1.6.1 [57] from GBDP distances calculated from 16S rDNA gene sequences showing the phylogenetic relationships between strain HM3 and the most closely related type strains of the genus Streptomyces. The branch lengths are scaled in terms of GBDP distance formula d5. Numbers above branches are GBDP pseudo-bootstrap support values > 60% from 100 replications, with an average branch support of 79.5%. The tree was rooted at the midpoint [58]. Bar, 0.002 substitutions per nucleotide position.

3.4. Overview of the Putative Secondary Metabolites' Biosynthetic Gene Clusters

To evaluate the potential biosynthetic gene clusters (BGCs) and their secondary metabolites, antiSMASH version 6.0 was used to predict both characterized and unknown putative secondary metabolites gene clusters in S. thinghirensis strain HM3. A total of 16 potential BGCs were predicted by antiSMASH with characterized functions (Table 3). These BGCs, including four terpene clusters, one lantipeptide cluster, one siderophore cluster, two PKS (polyketide synthase) clusters, two NRPS (non-ribosomal peptide synthetase cluster)/NRPS-like fragment clusters, two RiPP/RiPP-like (ribosomally synthesised and

post-translationally modified peptide product) clusters, two butyrolactone clusters, one CDPS (tRNA-dependent cyclodipeptide synthases) cluster, and one other (cluster containing a secondary metabolite-related protein that does not fit into any other category) BGC. The main BGC types in strain HM3 were terpene, PKS, NRPS, and butyrolactone.

Table 3. Possible secondary metabolites of S. thinghirensis strain HM3 based on genome analysis by antiSMASH.

Region (Contigs)	Type	Nucleotide Sequences (From–To)	Most Similar Known Cluster	Microorganism	Similarity Percentage	Reference
Region 2.1	Terpene	12,171–33,262	Albaflavenone	*Streptomyces coelicolor* A3(2)	100	[59]
Region 6.1	Terpene	8731–27,414	-	-	-	-
Region 17.1	Terpene	39,937–60,815	-	-	-	-
Region 50.2	Terpene	237,876–258,370	Hopene	*Streptomyces coelicolor* A3(2)	38	[60]
Region 8.1	Lantipeptide class V	75,517–117,727	Guadinomine (NRP + polyketide)	*Streptomyces* sp. K01-0509	7	[61]
Region 9.1	Siderophore	31,741–44,344	-	-	-	-
Region 15.1	Type II PKS (Polyketide synthase)	42,349–113,381	Xantholipin (Polyketide)	*Streptomyces flavogriseus*	8	[62]
Region 24.1	NRPS	19,390–61,821	Surugamide A/D (NRP)	*Streptomyces albidoflavus*	23	[63]
Region 35.1	RiPP-like	4066–14,248	Informatipeptin (RiPP: Lantipeptide)	*Streptomyces viridochromogenes* DSM 40736	28	[64]
Region 41.1	Butyrolactone	84,097–94,972	SCB1	*Streptomyces coelicolor* A3(2)	100	[65]
Region 54.1	Butyrolactone	33,375–44,304	Methylenomycin A	*Streptomyces coelicolor* A3(2)	9	[66]
Region 44.1	Type II PKS	44,648–107,146	Prejadomycin (Polyketide/ Saccharide)	*Streptomyces* sp. PGA64	41	[67,68]
Region 50.1	RiPP	159,658–179,906	SSV-2083 (RiPP:Lantipeptide)	*Streptomyces sviceus* ATCC 29083	27	[69]
Region 59.1	CDPS	1–13,469	-	-	-	-
Region 59.2	NRPS-like	104,234–151,246	Calyculin A (NRP + polyketide: Trans-AT type I)	Uncultured Candidatus *Entotheonella* sp.	28	[70,71]
Region 62.1	Other	18,773–59,354	Actinomycin D (NRP)	*Streptomyces anulatus*	57	[72–74]

3.5. BGCs Involving Terpene Biosynthesis

Based on the in silico analysis, the *S. thinghirensis* HM3 genome revealed four terpene gene clusters. The first gene cluster proposed to produce albaflavenone terpene, whose similarity reached 100% with albaflavenone from *Streptomyces coelicolor* A3(2) based on KnownClusterBlast (Figure 3A, Figure S2). This BGC was located in region 2.1 and spanned 21.09 kb in size. It contained up to twenty related genes (Figure 3B), including both core biosynthetic, tailoring enzymes, and regulatory genes which were predicted to be involved in albaflavenone terpene biosynthesis. Based on the MIBiG analysis, the main genes in this cluster were found to be terpene synthase family protein and cytochrome P450 (genes 11 and 12 in Figure 3B, respectively). The terpene synthase was predicted to catalyse the cyclization of farnesyl diphosphate to epi-isozizaene (the tricyclic hydrocarbon), whereas cytochrome P450 converts epi-isozizaene to the sesquiterpene antibiotic albaflavenone via carrying out two sequential allylic oxidations. Notably, the Pfam domains analysis revealed that more than fifteen genes could contribute to albaflavenone biosynthesis (Figure 3C).

The second terpenes gene cluster existed in region 50.2 and spanned 20.5 kb in size, with 38% similarity to the hopene biosynthetic gene cluster from *S. coelicolor* A3(2) when compared at KnownClusterBlast (Figures 4A and S3). This BGC had up to twenty genes encoding terpene biosynthesis (Figure 4B,C). The first part of the cluster was involved in the 2-C-methyl-D-erythritol 4-phosphate (MEP) pathway. The putative 1-deoxy-D-xylulose-5-phosphate synthase (gene 1) was predicted to biosynthesis 1-deoxy-D-xylulose 5-phosphate (DXP) from pyruvate and methylerythritol 2,4-cyclodiphosphate (MEcDP) to be converted into hydroxymethylbutenyl diphosphate (HMBDP) by HMBDP synthase (gene 2); then, HMDBP would be reduced to isopentenyl diphosphate (IPP) by HMBDP reductase (gene 5). Otherwise, the second part of the cluster was predicted to participate in squalene and hopene biosynthesis (genes 4, 6, 7, 8, 9, 10, 11, 12 and 13) with genes encoding squalene-hopene cyclase C/N-terminal domains, polyprenyl synthetase, hydroxysqualene dehydroxylase HpnE and squalene/phytoene synthase, respectively (Figure 4B,C). Furthermore, another two BCGs related to terpenes were detected in regions 6.1 and 17.1,

ranging in size from 18.6 to 20.88 kb, respectively (Table 2). Based on genetic similarity and organization at MIBiG, the first BGC's similarity score reached 0.24 with the carotenoid terpene from *Myxococcus xanthus*, whereas the second cluster exhibited 0.56 similarity with the geosmin terpene from *S. coelicolor* A3(2).

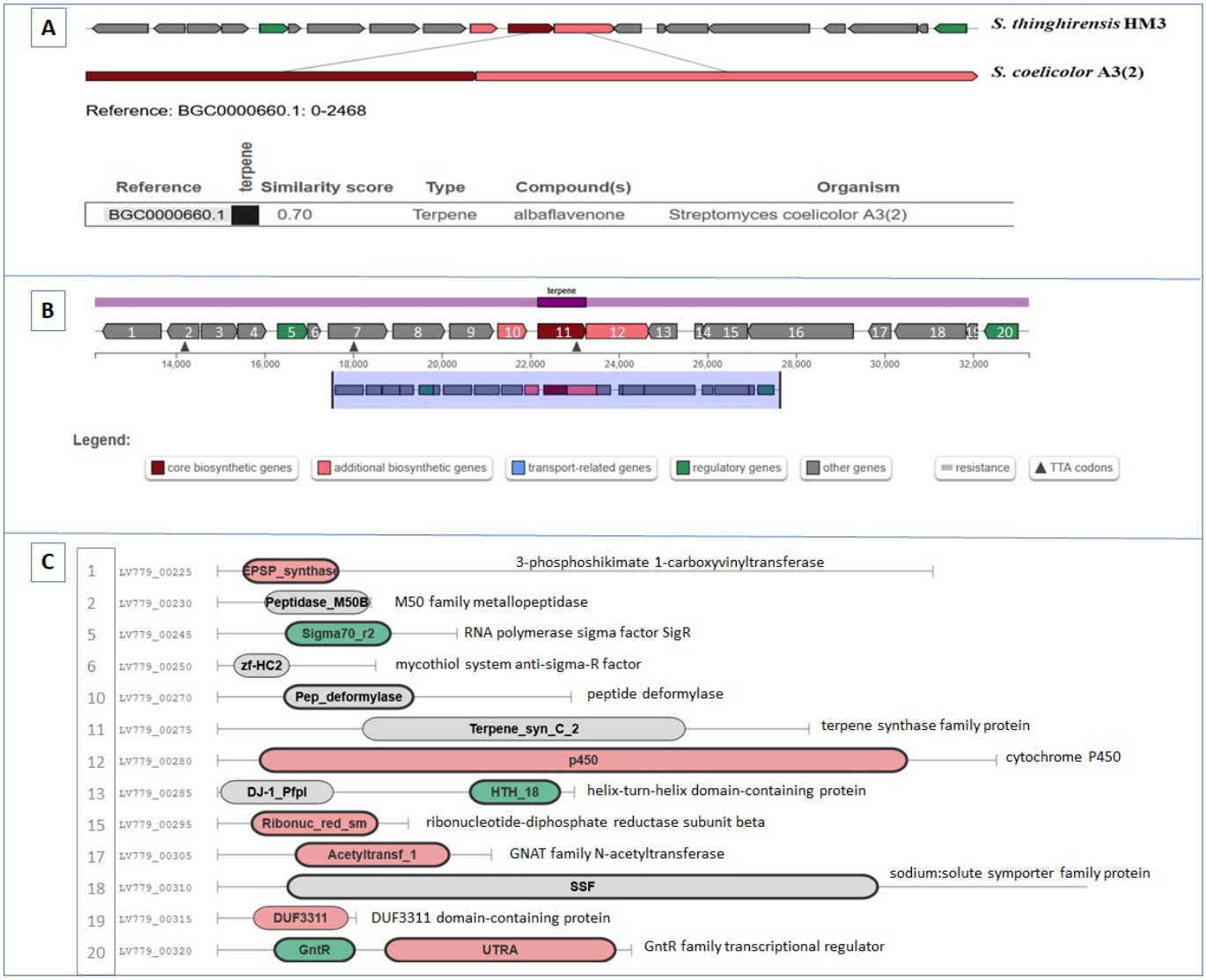

Figure 3. Terpene (albaflavenone) biosynthetic gene cluster in *S. thinghirensis* HM3. (**A**) The comparison between the proposed albaflavenone gene cluster (dark red gene) in strain HM3 and the proposed identified cluster of albaflavenone in *S. coelicolor* A3(2) with a similarity score of 0.7 on the MIBiG website. (**B**) The proposed albaflavenone gene cluster in region 2.1 from strain HM3 genome; 3, SOS response-associated peptidase; 4, hydrolase; 7, HD-GYP domain-containing protein; 8, metal-dependent phosphohydrolase; 9, 14 hypothetical protein; 16, ribonucleoside-diphosphate reductase subunit alpha. (**C**) represents the predicted genes involved in albaflavenone biosynthesis based on the Pfam website.

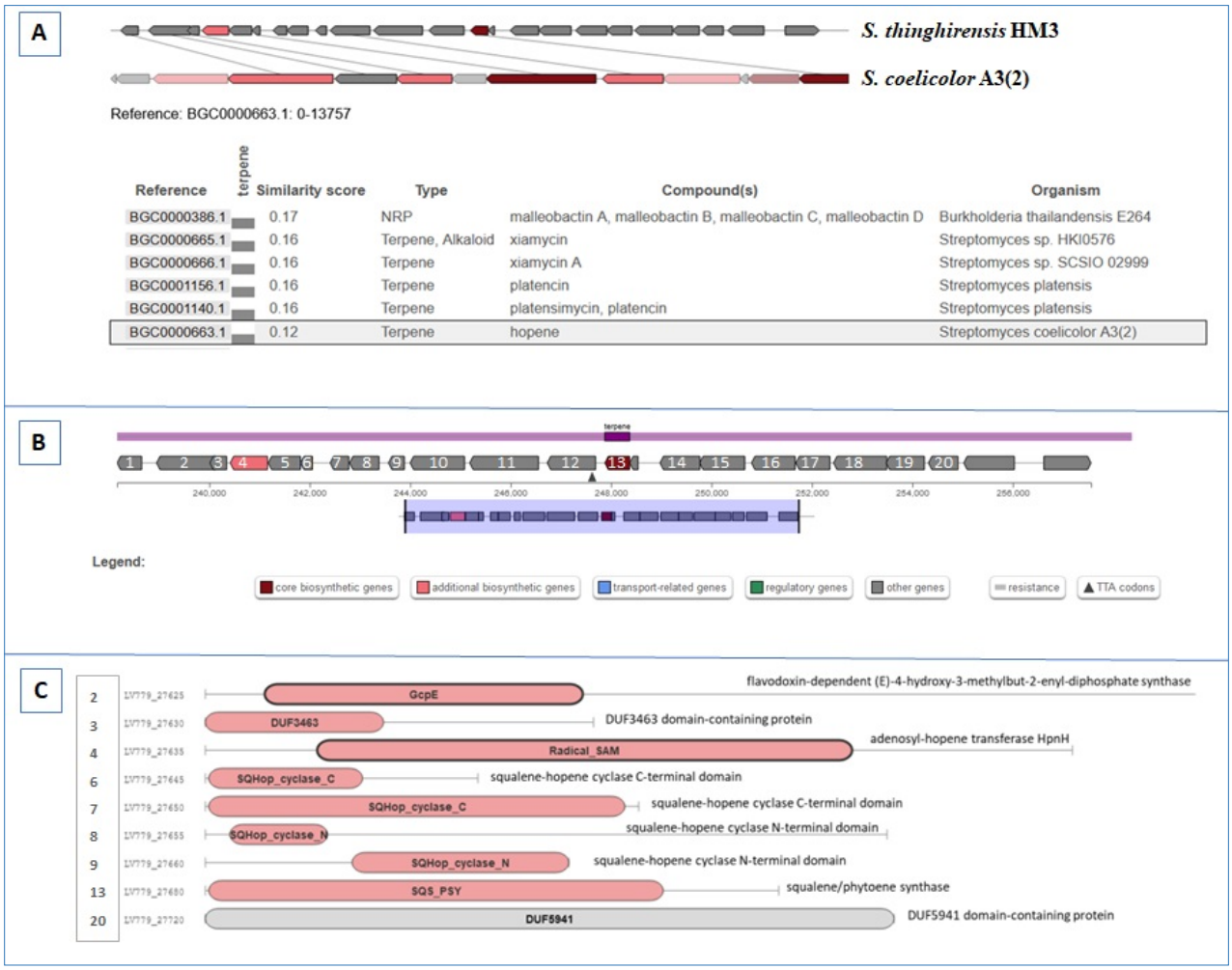

Figure 4. Terpene (hopene) biosynthetic gene cluster in *S. thinghirensis* HM3. (**A**) The comparison between the proposed hopene gene cluster (dark red gene) in strain HM3 and the proposed identified cluster of hopene in *S. coelicolor* A3(2) with a similarity score of 0.12 on the MIBiG website. (**B**) The proposed hopene gene cluster in region 50.2 from strain HM3 genome contains; 1, 1-deoxy-D-xylulose-5-phosphate synthase; 5, 1-hydroxy-2-methyl-2-butenyl 4-diphosphate reductase; 10, polyprenyl synthetase; 11, hydroxysqualenedehydroxylaseHpnE; 12, squalene/phytoene synthase; 14, ABC transporter ATP-binding protein; 15, ABC transporter permease; 16, glycosyltransferase; 17, CDP-alcohol phosphatidyltransferase; 18, iron-containing alcohol dehydrogenase; 19, phosphocholine cytidylyltransferase. (**C**) represents the predicted genes involved in hopene biosynthesis based on the Pfam website.

3.6. BGCs Involving NRPS, PKS, and NRPS/PKS Hybrid

A total of five putative antiSMASH-identified NRPS, PKS, NRPS/PKS Hybrid, and Lanthipeptide BGCs were identified to be distributed in the genome. The NRPS BGC was located in region 24.1, was 42,4 kb in size, and was predicted to produce the cyclic octapeptides surugamide A/D or vulnibactin based on domain composition and organization analysis at MIBiG or KnownClusterBlast (Figure 5A, Figure S4). In this cluster, more than 28 genes may be involved in the biosynthetic process (Figure 5B,C) with multiple condensation domains (C), amino acid adenylation domains (A), phosphopantetheine-binding protein (PP), acyl carrier protein (AC), thioesterase domain (TE), and ketoreductase (KR).

Figure 5. NRPS biosynthetic gene cluster in *S. thinghirensis* HM3. (**A**) The comparison between the proposed NRPS gene cluster in strain HM3 and the proposed identified cluster of vulnibactin in *Vibrio vulnificus* CMCP6 with a similarity score reaching 0.29 on the MIBiG website. (**B**) The proposed NRPS gene cluster in region 24.1 of strain HM3 genome; 1, 6 and 8, AMP-binding protein; 10, MbtH family NRPS accessory protein; 11, FtsX-like permease family protein; 12, ABC transporter permease; 13, ABC transporter ATP-binding protein; 14, 15, MFS transporter; 16, ornithine carbamoyltransferase; 20, 21, 2,3-diaminopropionate biosynthesis protein SbnB/SbnA; 22, condensation domain; 25, 26, TauD/TfdA family dioxygenase. (**C**) represents the NRPS domains involved in NRPS biosynthesis with predicted chemical structure based on PRISM.

The NRPS-like fragment/transAT-PKS-like was classified as a hybrid cluster (Figure 6) in region 59.2 with nucleotides sized at 47 kb. This BCG showed up to a 0.51 and 0.49 similarity score with massetolide A (the cyclic lipopeptide (CLP) antibiotic) and caboxamycin (a new benzoxazole antibiotic) from *Pseudomonas fluorescens* SS101 and *Streptomyces* sp. NTK 937, respectively, on the MIBiG database. When compared at KnownClusterBlast, 28%, 40%, and 57% similarities with calyculin A (a biosynthetic gene cluster from uncultured *CandidatusEntotheonella* sp.), swinholide A (a biosynthetic gene cluster from *Nostoc* sp. UHCC 0450), and oxazolepoxidomycin (a biosynthetic gene cluster from *Streptomyces* sp. NRRL F-4335), were detected (Figure S5). The BCG contained genes involved in the biosynthetic process (Figure 6C). In addition, further genes may participate in the production process (Figure 6B).

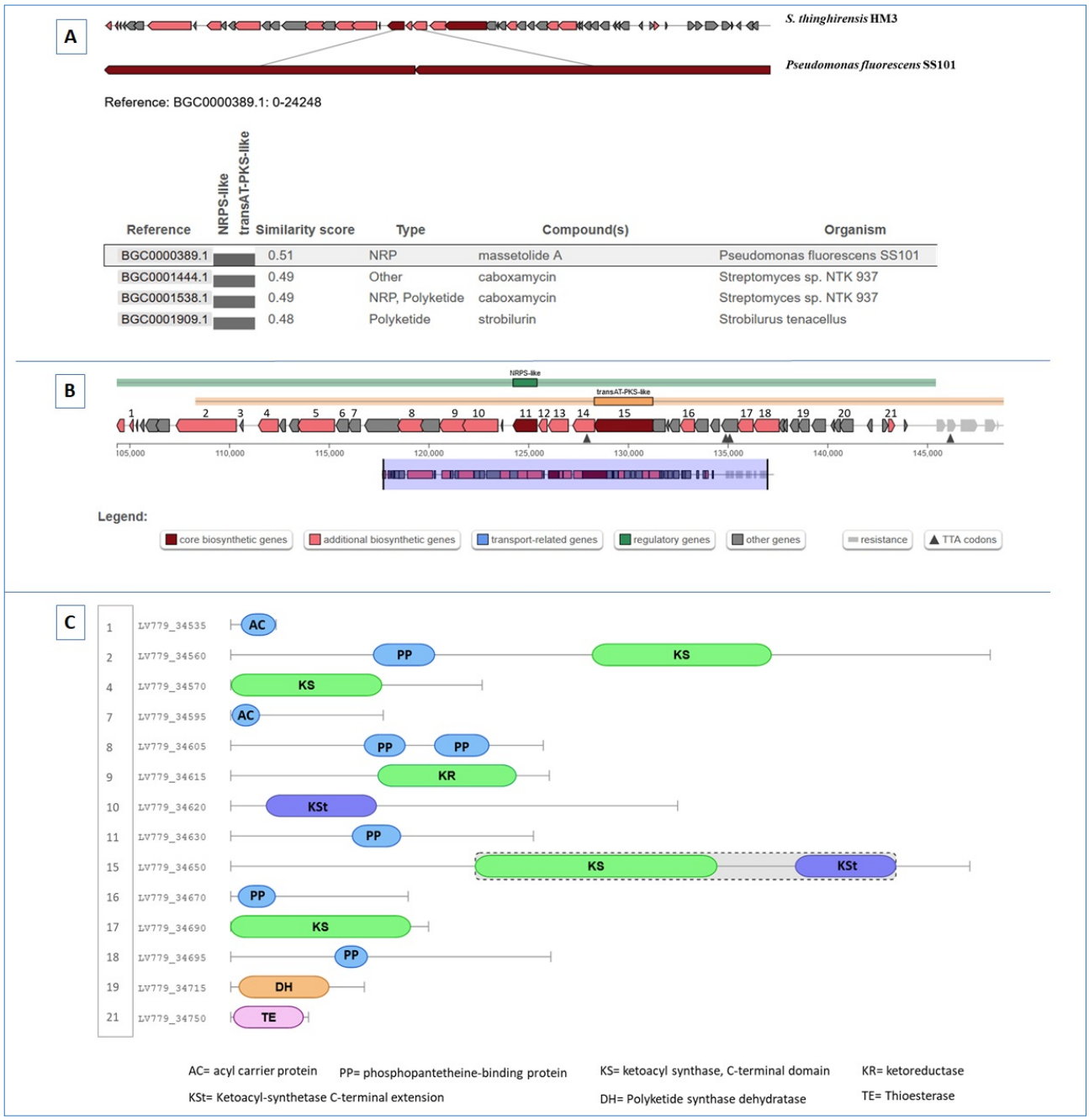

Figure 6. NRPS-like fragment/transAT-PKS-like biosynthetic gene cluster in *S. thinghirensis* HM3. (**A**) The comparison between the proposed NRPS-like fragment/transAT-PKS-like gene cluster in strain HM3 and the proposed identified cluster of massetolide A and caboxamycin in *Pseudomonas fluorescens* SS101 and *Streptomyces* sp. NTK 937 had a similarity score reaching 0.51 and 0.49 at MIBiG website. (**B**) The proposed NRPS-like fragment/transAT-PKS-like gene cluster in region 59.2 of strain HM3 genome; 3, KR domain-containing protein; 5, hypothetical protein; 6, 14, condensation domain; 12, 13, AMP-binding protein; 20, polyketide synthase. (**C**) represents the domains involved in NRPS-like fragment/transAT-PKS-like biosynthesis based on Pfam.

As for PKS BGCs, two clusters related to type II PKS were identified by antiSMASH. The first cluster existed in region 15.1 and exhibited 8% and 19% shared sequences with xantholipin (a polycyclic xanthone antibiotic with antimicrobial and antitumour activities) from *Streptomyces flavogriseus*, and mensacarcin (a potential antitumour drug) from *Streptomyces bottropensis*, when compared with KnownClusterBlast. The second type II PKS BCG

spanned 44,648 to 107,146 (with approximately 62.5 kb in region 44.1). Retrieved data from the MIBiG comparison showed a similarity score of 0.61 and 0.59 with griseusin (pyranonaphthoquinone antibiotic) and jadomycin (angucycline polyketide antibiotic) from *S. griseus* and *S. venezuelae* ATCC 10712, respectively (Figure 7). Furthermore, 41% of the shared sequences were detected with prejadomycin biosynthetic gene cluster from *Streptomyces* sp. PGA64 as a KnownClusterBlast (Figure 6S). The domain composition and organization of the identified type II PKS cluster is summarized in Figure 7. Notably, the cluster contained up to forty genes predicted to participate in the biosynthetic process (Figure 7B). The main domains are presented in Figure 7C,D.

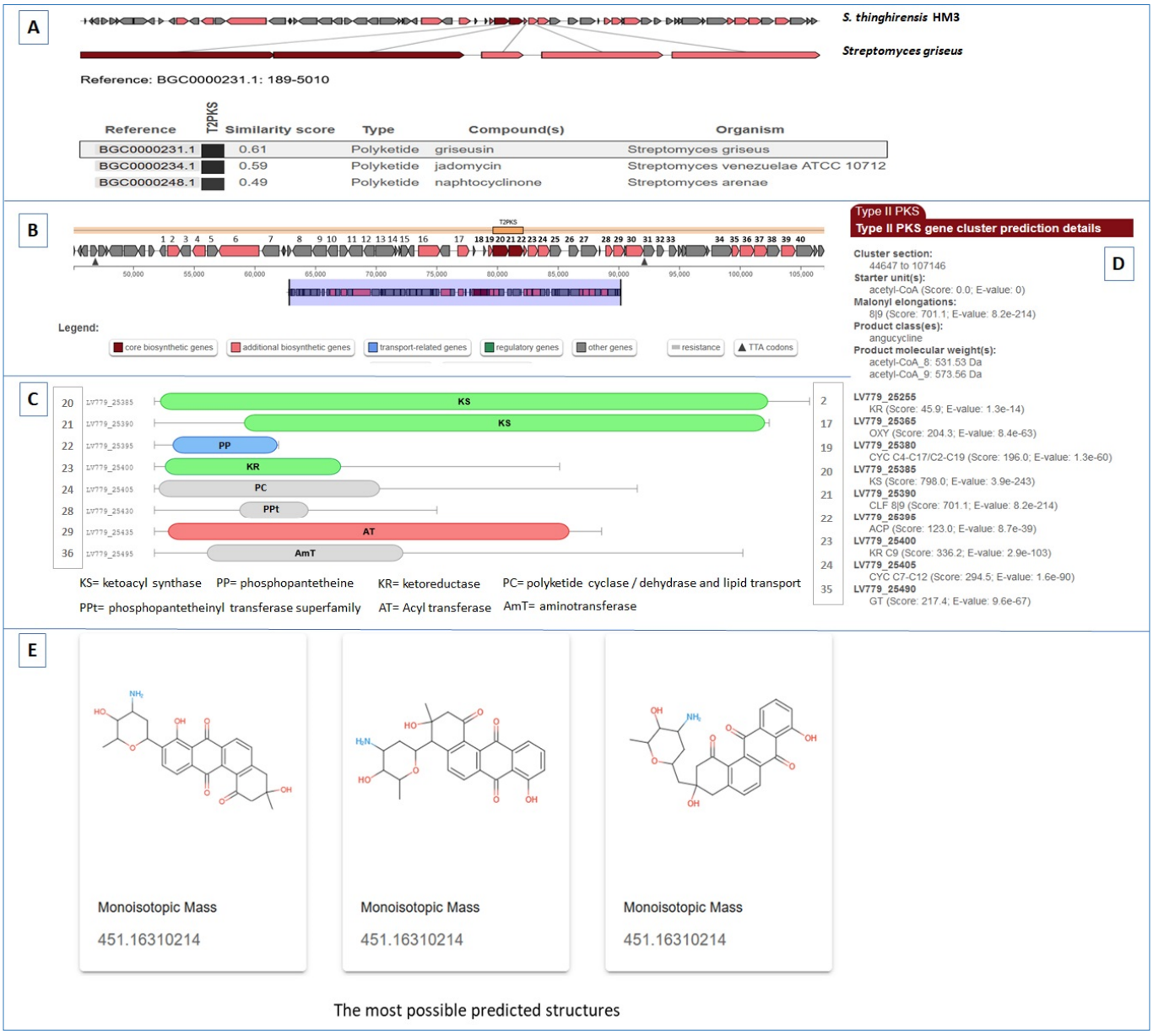

Figure 7. Type II PKS biosynthetic gene cluster in *S. thinghirensis* HM3. (**A**) The MIBiG comparison between the proposed Type II PKS BGC in strain HM3 and the proposed identified cluster of griseusin and jadomycin in *S. griseus* and *S. venezuelae* ATCC 10712, with a similarity score reaching 0.61 and 0.59. (**B**) The proposed type II PKS BGC in region 44.1 of strain HM3 genome. (**C**,**D**) represent the domains involved in PKS biosynthesis. (**E**) represents the most possible predicted chemical structures based on PRISM.

3.7. Gene Clusters Involving RiPP, Butyrolactone, and Other Biosynthesis

The RiPP cluster (region 50.1 in the genome) was homologous to the citrulassin E (a lasso peptide) cluster from *S. glaucescens* (Figure 8). This homologous was calculated at 27% and 50% with the SSV-2083 biosynthetic gene cluster from *S. sviceus* ATCC 29083, and the moomysin (the class II lasso peptides) biosynthetic gene cluster from *S. cattleya* NRRL 8057, respectively (Figure S7). The predicted first step was the lasso RiPP family leader peptide-containing protein (gene 4, Figure 8B) that binds the precursor peptide and directs further enzymatic modifications. More genes are necessary to install the post-translational modifications, i.e., asparagine synthase (gene 5, homologous to lasso cyclase) was predicted to catalyse isopeptide bond formation in macrocycle creation between the N-terminus and the carboxyl side chain of a Asp or Glu residue within the core region. PqqD-protein (gene 6, peptide chaperone) was predicted to be involved in the maturation of lasso peptides. Additional genes coding for transport systems (genes 7 and 8) existed in the pathway. Various auxiliary genes predicted to code for extra modification enzymes, such as GNAT family N-acetyltransferase, cupin domain-containing protein, and Gfo/Idh/MocA family oxidoreductase (genes 10, 11, and 12), were found in the lasso-cluster.

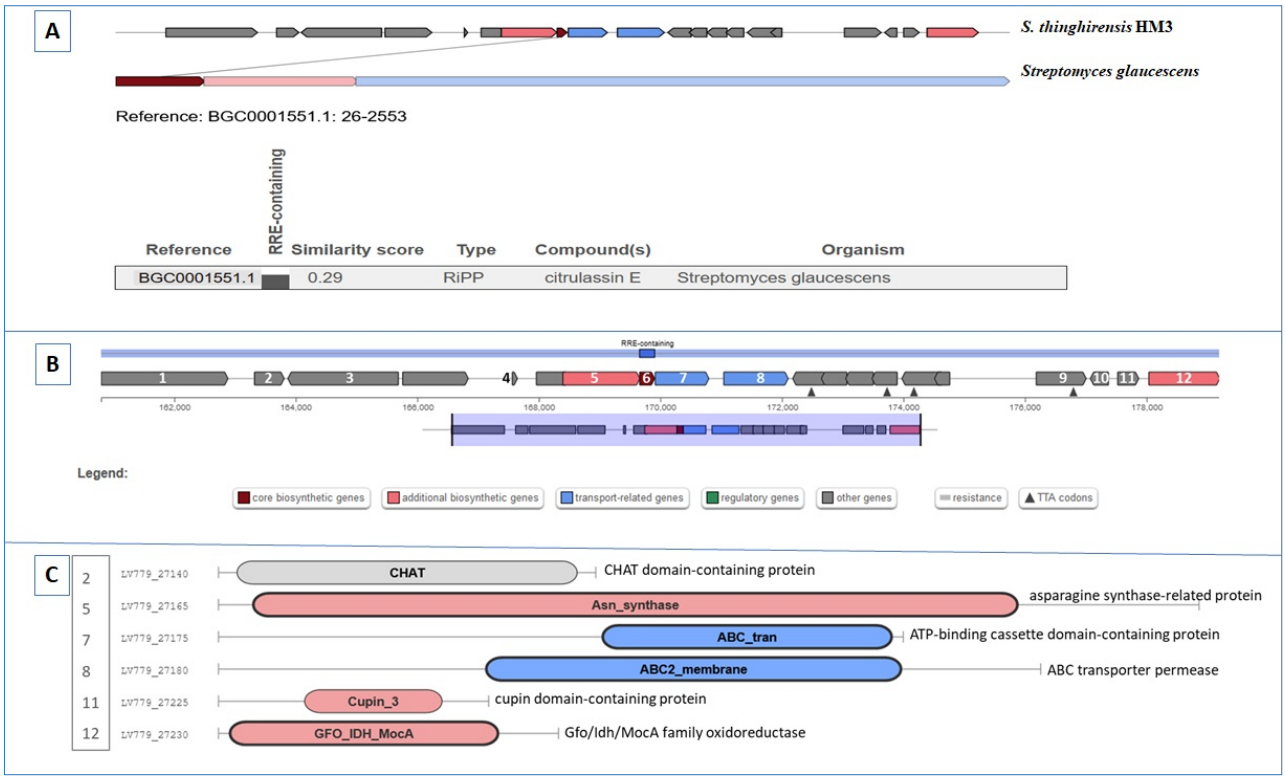

Figure 8. RiPP biosynthetic gene cluster in *S. thinghirensis* HM3. (**A**) The MIBiG comparison between the proposed RiPP BGC in strain HM3 and the proposed identified cluster of citrulassin E in *S. glaucescens* with a similarity score of 0.29. (**B**) The proposed RiPP BGC in region 50.1 of the genome; 1, tetratricopeptide repeat protein; 3, LuxR C-terminal-related transcriptional regulator; 4, lasso RiPP family leader peptide-containing protein; 6, PqqD family protein; 9, bile acid:sodium symporter family protein; 10, GNAT family N-acetyltransferase. (**C**) represents the Pfam domains involved in RiPP biosynthesis.

According to our in silico analysis, two possible butyrolactones were present in the genome, with similarity reaching 100% and 12% according to KnownClusterBlast (Figure S8). In the MIBiG comparison, the first BGC exhibited a score of 0.45 with the SCB1 biosynthetic gene cluster from *S. coelicolor* A3(2) (Figure 9). Genes 4 and 5 were predicted to encode the A-factor biosynthesis hotdog domain (catalyses transfer of beta-ketoacyl from

8-methyl-3-oxononanoyl-acyl carrier protein to the hydroxyl group of dihydroxyacetone phosphate (DHAP), and subsequently, to produce an 8-methyl-3-oxononanoyl-DHAP ester). Gene 6 was predicted to be a NAD(P)H-binding protein with NAD(P)H-dependent reductase activity, while gene 8 is proposed to be a gamma-butyrolactone binding protein (ATP-binding protein) with regulation function.

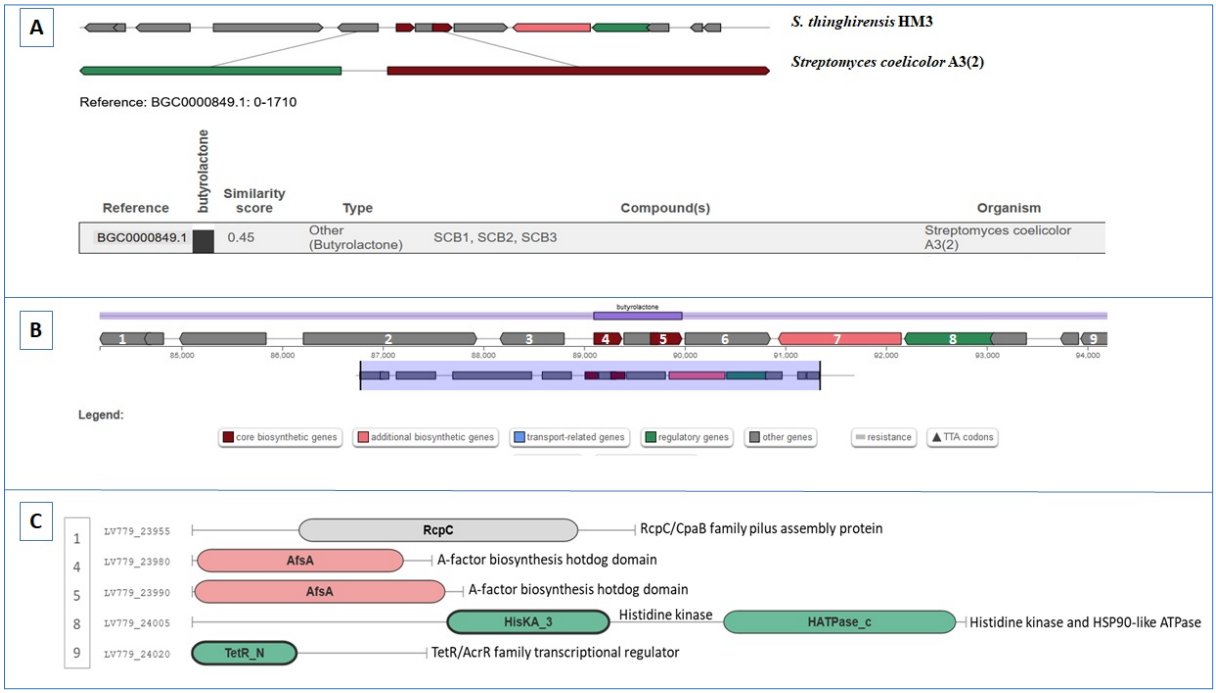

Figure 9. Butyrolactone biosynthetic gene cluster in *S. thinghirensis* HM3. (**A**) The MIBiG comparison between the proposed butyrolactone BGC in strain HM3 and the proposed identified cluster of SCB1 in *S. coelicolor* A3(2) recorded a similarity score of 0.45. (**B**) The proposed butyrolactone BGC in region 41.1 of the genome; 2, glycoside hydrolase family 18 protein; 3, TetR/AcrR family transcriptional regulator; 6, NAD(P)H-binding protein; 7, cytochrome P450. (**C**) represents the Pfam domains involved in butyrolactone biosynthesis.

The last identified BGC was classified as other (cluster containing a secondary metabolite-related protein that does not fit into any other category) in region 62.1, with a length calculated to be 40.58 kb. Based on the antiSMASH analysis, the identified cluster showed high homology (57%) with the known BGC of actinomycin D from *S. anulatus* (Figure S9). The proposed cluster contained more than twenty-four genes that may be involved in the biosynthetic process (Figure 10). The main genes in the biosynthetic process were tryptophan 2,3-dioxygenase family protein (gene 17), kynureninase (gene 16, a hypothetical protein showing 72% identity with kynureninase from *S. anulatus*), and methyltransferase domain-containing protein (gene 15), which were considered to be involved in the conversion of tryptophan to 4-Methyl-3-hydroxy-anthranilic acid (4-MHA). Furthermore, peptide synthetase genes with amino acid adenylation domain-containing protein (gene 21), thioesterase domain (gene 18), condensation domain (genes 24 and 27), phosphopantetheine-binding protein (genes 19 and 25), and AMP-binding protein (genes 1, 22, 23, 26 and 27), are mandatory for the biosynthetic process. Axillary genes related to regulation (i.e., TetR/AcrR family transcriptional regulator, LmbU family transcriptional regulator (genes 11 and 12) and transport (i.e., excinuclease ABC subunit UvrA, ABC transporter permease, and ATP-binding cassette domain-containing protein (genes 6, 7, and 9)) were detected in the cluster. Cytochrome P450 (gene 14) would hydroxylate proline in actinomycin $X_{o\beta}$ production.

Figure 10. The proposed actinomycin D biosynthetic gene cluster in *S. thinghirensis* HM3. (**A**) The MIBiG comparison between the proposed BGC in strain HM3 and the proposed identified cluster of fellutamide B in *Aspergillus nidulans* FGSC A4, with a similarity score of 0.31. (**B**) The proposed actinomycin D-BGC in region 62.1 of the genome; 5, ANTAR domain-containing protein; 6, excinuclease ABC subunit UvrA; 7, ABC transporter permease; 12, LmbU family transcriptional regulator; 14, cytochrome P450; 15, methyltransferase domain-containing protein; 16, aminotransferase; 19, phosphopantetheine-binding protein; 20, alpha/beta fold hydrolase. (**C**) represents the Pfam domains involved in actinomycin D biosynthesis.

4. Discussion

Natural products produced by microorganisms are a precious source of bioactive molecules and natural antibiotics with pharmaceutical applications. Microorganisms produce these compounds that allow them to interact and survive in adverse environments [75]. *Streptomyces* bacteria are broadly recognized as the most notable organisms for natural products production [6,11,13,18,23]. Novel antibiotics are urgently required to face the global crisis of drug resistance. The presence and source of carbon is an essential element in secondary metabolites production. Genome mining enables the link between the proposed secondary metabolites and their respective biosynthetic genetic clusters [76–80]. The physicochemical properties of soil affect the microbial communities, and subsequently, the accumulation of secondary metabolites. In sandy clay, the accumulation of secondary metabolites by *Bletilla striata* was significantly higher, but this improved in sandy loam soil [76].

S. thinghirensis HM3 isolated from Qassim, SA, exhibited antibacterial and antifungal efficiency; subsequently, it was subjected to genome sequencing. A total of 30,937 reads were generated with a read length reaching 44,764,953 bp. The genome length was recorded as 7,14 Mbp with an average GC content of 71.49%. The bacterial genome contained 7949 gene sequences, 3362 protein-coding sequences, 12 complete rRNA genes, and 60 tRNAs. *Streptomyces* sp. MP131-18, isolated from a marine sediment sample in Norway, implied 72.4% G+C content, 7054 proteins, and 78 tRNA-encoding genes [80]. Moreover, Lee et al. [81] presented the genome sequences of 8 *Streptomyces venezuelae* and 22 *Streptomyces* species. The total genome lengths ranged from 6.7 to 10.1 Mbp with 7000 protein-coding genes, 20 rRNAs, and 68 tRNAs on average.

S. thinghirensis HM3 exhibited patterns of antifungal and antibacterial activities. Based on previous research, the HM3 strain revealed antagonism with seven different soil-borne fungi [34]. Moreover, it showed antibacterial inhibitory effect against Gram-positive bacteria, including *S. pneumoniae* ATCC 49619, *S. aureus* ATCC 29213, and MRSA-A. Jaroszewicz et al. [82] isolated two new *Streptomyces* sp. strains with the ability to inhibit the growth of fungi (different species of genus *Candida*) and pathogenic bacteria (i.e., *Salmonella enterica*, *Pseudomonas aeruginosa*. *Staphylococcus aureus*, *Enterococcus* sp., and *Escherichia coli*), while Kim et al. [83] isolated *S. blastmyceticus* 12-6 with strong antifunal activity against *Colletotrichum acutatum*, *C. gloeosporioides*, *C. coccodes*, *Trichothecium roseum*, and *Fusarium oxysporum*.

Moreover, *S. griseoaurantiacus* AD2, isolated from honey, displayed an inhibitory effect with Gram-positive pathogenic bacteria, such as *Enterococus faecalis* and *Staphylococcus aureus* [84]. *Streptomyces* sp. AN090126 excreted streptomycin sulphate with an inhibition effect against streptomycin-resistant *Pectobacterium carotovorum* subsp. *Carotovorum*, whereas *Streptomyces* sp. strains IBSBF 2397 and IBSBF 2019 were able to inhibit the growth of Gram-positive and Gram-negative bacteria, *Bacillus cereus* (ATCC 14579), *E. coli* (ATCC 11775), *Staphylococcus aureus* (ATCC 25923), and *Pseudomonas aeruginosa* (ATCC 27853) [85,86].

The in silico prediction of SM-BGCs (secondary metabolite biosynthetic gene clusters) by antiSMASH and PRISM identified 16 potential BGCs in the HM3 genome. These BGCs included terpenes, lantipeptide, siderophore, PKS, NRPS, RiPP/RiPP-like, butyrolactone, CDPS, and others. *Streptomyces formicae* KY5 revealed various secondary metabolites encoded by BGCs, i.e., 2 PKS potentially encodes formicamycins, 11 NRPS, and 6 terpenes (two clusters were predicted to encode siderophore-like desferrioxamine, whereas another terpene potentially produces albaflavenone antibiotic) [87]. Applying the same method (antiSMASH analysis) of prediction with *Streptomyces* sp. MP131-18 revealed 36 gene clusters involved in possible secondary metabolites production. Five gene clusters predicted to encode terpenes (six gene clusters with type I polyketide synthase (PKS), three non-ribosomal peptide synthase (NRPS) gene clusters, a large group of RiPPs (ribosomally synthesized and post-translationally modified peptides), two siderophore molecules, melanine, ectoine, bacteriocin, and A-factor-like butyrolactone) were found within the genome [80]. Komaki et al. [88] reported three type I PKS, seven NRPS, and four hybrid PKS/NRPS gene clusters responsible for rakicidin synthesis inside the draft genome sequence of *Streptomyces* sp. MWW064 (NBRC 110611).

Terpenes are considered the most diverse and abundant class of natural products. They can be used in various application such as fragrances, flavours, pharmaceuticals, biofuel precursors, and as pesticides in agriculture [89–92]. Four terpene gene clusters were identified in the *S. thinghirensis* HM3 genome. The first cluster was proposed to produce albaflavenone terpene, with similarity reaching 100% with albaflavenone from *Streptomyces coelicolor* A3(2). The second terpene cluster showed similarity measured at 38% with a hopene cluster from *S. coelicolor* A3(2). The other two terpenes showed low similarity with a carotenoid from *Myxococcus xanthus* and geosmin from *S. coelicolor* A3(2). Usually, terpenes are biosynthesized from isopentenyl diphosphate (IPP) and dimethylallyl diphosphate (DMAPP) (universal precursors with C5). A condensation process with, for example, the prenyltransferases assembly of two or more IPP and DMAPP in a "head-

to-tail" fashion, leads to the formation of linear prenyl diphosphate compounds such as geranyl diphosphate (GPP, C10), farnesyl diphosphate (FPP, C15), or geranylgeranyl diphosphate (GGPP, C20). These formed compounds represent a precursors pool which can be used by the terpene synthases for different terpenoid biosynthesis [89,90]. For example, a head-to-head style condensation of FPP and GGPP can form, for example, squalene, dehydro-squalene (DHS), or phytoene, which are the precursors of hopanoids (bacteriohopanetetrol), sterols (cholesterol), and carotenoids (β-carotene) [93,94].

Polyketide synthases (PKS) and nonribosomal peptide synthetases (NRPS) are involved in the synthesis of the PKs/NRPs compounds (polymers of carbonyl/peptidyl chains). The BGCs related to PKS and NRPS encode modular enzymes containing modules. Additionally, the NRPS enzyme contains three domains: a peptidyl carrier protein (PCP) with a phosphopantetheine group/the thiolation (T) domain, which is necessary for the binding and transfer of the adenylated monomer; an AMP-binding (A) domain with the selection and activation function of an amino acid; and a condensation (C) domain with peptide bond formation and elongation function. Moreover, additional domains could be involved, such as dehydratases (DH) and ketoreductases (KR) for chain post-extensional modifications, while the thioesterase (TE) domain participates the in cycling and release of the mature chain [95–99]. The basic PKS module consists of an acyl carrier protein (ACP) domain with a phosphopantetheinyl arm, an acyltransferase (AT) domain for the selection and transfer of carboxylic acid, and a beta-keto synthase (KS) domain with a decarboxylative condensation function. PKS pathways can be divided into three types: type I PKS, type II PKS, and type III PKS [95–97,100]. RiPPs represent promising alternative antimicrobial peptides which are divided into subfamilies based on their structural composition and biosynthetic enzymes. These RiPPs include compounds such as lasso peptides, bacteriocins, lantipeptides, and thiopeptides [95,101].

The *S. thinghirensis* HM3 genome encodes numerous PKS, NRPS, NRPS/PKS hybrid, RiPP, RiPP-like, butyrolactone, lantipeptide, and other gene clusters, which may assist the bacterium in its fight against predators and competitors existing in its environment. The gene clusters involved in the biosynthesis of natural products usually contain core biosynthetic and tailoring enzymes, in addition to regulator genes that regulate the biosynthesis process. Furthermore, export/transport genes such as efflux pumps, which export the produced product to the extracellular environment, are known to exist. Komaki and Tamura [102] explored the whole genome of four *Phytohabitans* (belonging to rare actinomycetes) regarding both PKS and NRPS gene clusters. Fifty-six PKS and NRPS gene clusters were detected via the bioinformation analysis of the entire four genomes.

Bacteria are familiar with antibiotic resistance originating from their protective outer membranes and the active efflux pumps that work constitutively. In turn, in this study, the representative *S. thinghirensis* HM3 produced probable bioactive compounds against both Gram-positive bacteria and soil-borne disease fungi, suggesting its potential utility as an antibacterial and antifungal agent. Strain HM3 may contribute to the development of a novel antibiotic against bacteria and fungi [103]. Qureshi et al. [40] isolated *Streptomyces smyrnaeus* UKAQ_23 from mangrove sediment. This strain exhibited antimicrobial activity against MRSA and non-MRSA Gram-positive bacteria as a result of actinomycin X_2 and actinomycin D production.

5. Conclusions

New natural products with bioactivity as secondary metabolites are necessary in current times. *S. thinghirensis* HM3 showed antibacterial and antifungal properties that suggest the production of potential secondary metabolites. The *S. thinghirensis* strain HM3 genome was sequenced by Oxford Nanopore technology. An antiSMASH and PRISM analysis of the genome exhibited 16 potential BGCs, such as four terpene clusters, two PKS clusters, two NRPS/NRPS-like fragment clusters, two RiPP/RiPP-like clusters, two butyrolactone clusters, one lantipeptide cluster, one siderophore cluster, one CDPS cluster,

and one other BGC. A potential new source of secondary metabolites could be attributed to *S. thinghirensis* strain HM3.

Supplementary Materials: The following supporting information can be downloaded at: https://www.mdpi.com/article/10.3390/fermentation9010065/s1, Figure S1: Tree inferred with FastME 2.1.6.1 in TYGS database from GBDP distances calculated from genome sequences (NCBI GenBank accession ID JAKFGP000000000) showing the phylogenetic relationships between strain HM3 and the most closely related type strains of the genus Streptomyces. The branch lengths are scaled in terms of GBDP distance formula d5. The numbers above the branches are GBDP pseudo-bootstrap support values > 60% from 100 replications, with an average branch support of 92.2%. Figure S2: Terpene (albaflavenone), KnownClusterBlast, and ClusterBlast. Figure S3: Terpene (hopene), KnownClusterBlast, and ClusterBlast. Figure S4: Non-ribosomal peptide synthetase cluster (NRPS), KnownClusterBlast, and ClusterBlast. Figure S5: NRPS-like fragment/transAT-PKS-like, KnownClusterBlast, and ClusterBlast. Figure S6: Type II PKS BCG based on KnownClusterBlast and Pfam domains. Figure S7: Ribosomally synthesised and post-translationally modified peptide product (RiPP) cluster/lanthipeptide, KnownClusterBlast. Figure S8: Butyrolactone cluster, KnownClusterBlast. Figure S9: Other, cluster containing a secondary metabolite-related protein that does not fit into any other category (actinomycin D), KnownClusterBlast.

Author Contributions: Conceptualization, M.R. and A.G.; methodology, M.R., A.G. and A.A.; software, M.R. and A.G.; formal analysis, A.A.; investigation, M.R., A.G. and A.A.; writing—original draft preparation, M.R. and A.G.; writing—review and editing, M.R., I.B.A. and A.G. All authors have read and agreed to the published version of the manuscript.

Funding: This research was funded by the Deputyship for Research & Innovation, Ministry of Education, Saudi Arabia, through the project number (QU-IF-4-1-4-30379).

Institutional Review Board Statement: Not applicable.

Informed Consent Statement: Not applicable.

Data Availability Statement: All data are available in the main text and Supplementary Materials.

Acknowledgments: The authors extend their appreciation to the Deputyship for Research & Innovation, Ministry of Education, Saudi Arabia, for funding this research work through the project number (QU-IF-4-1-4-30379). The authors also thank Qassim University for technical support. Authors thank Louis Tisa, University of New Hampshire, USA, for the manuscript English revision and correction.

Conflicts of Interest: The authors declare no conflict of interest.

References

1. Waksman, S.A.; Henrici, H.T. The Nomenclature and Classification of the Actinomycetes. *J. Bacteriol.* **1943**, *46*, 337–341. [CrossRef] [PubMed]
2. Dewi, T.K.; Agustiani, D.; Antonius, S. Secondary Metabolites Production by Actinomycetes and Their Antifungal Activity. *KnE Life Sci.* **2017**, *3*, 256–264. [CrossRef]
3. Lacey, H.J.; Rutledge, P.J. Recently Discovered Secondary Metabolites from *Streptomyces* Species. *Molecules* **2022**, *27*, 887. [CrossRef] [PubMed]
4. Salwan, R.; Sharma, V. Chapter 15—Bioactive Compounds of *Streptomyces*: Biosynthesis to Applications. In *Studies in Natural Products Chemistry*; Atta-Ur-Rahman, M., Ed.; Elsevier: Amsterdam, The Netherlands, 2020; Volume 64, pp. 467–491, ISBN 1572–5995.
5. Selim, M.S.M.; Abdelhamid, S.A.; Mohamed, S.S. Secondary Metabolites and Biodiversity of Actinomycetes. *J. Genet. Eng. Biotechnol.* **2021**, *19*, 72. [CrossRef]
6. Ahsan, T.; Chen, J.; Zhao, X.; Irfan, M.; Wu, Y. Extraction and Identification of Bioactive Compounds (Eicosane and Dibutyl Phthalate) Produced by *Streptomyces* Strain KX852460 for the Biological Control of Rhizoctonia Solani AG-3 Strain KX852461 to Control Target Spot Disease in Tobacco Leaf. *AMB Express* **2017**, *7*, 54. [CrossRef] [PubMed]
7. Stackebrandt, E.; Rainey, F.A.; Ward-Rainey, N.L. Proposal for a New Hierarchic Classification System, Actinobacteria Classis Nov. *Int. J. Syst. Evol. Microbiol.* **1997**, *47*, 479–491. [CrossRef]
8. Kämpfer, P.; Glaeser, S.P.; Parkes, L.; van Keulen, G.; Dyson, P. *The Family Streptomycetaceae BT—The Prokaryotes: Actinobacteria*; Rosenberg, E., DeLong, E.F., Lory, S., Stackebrandt, E., Thompson, F., Eds.; Springer: Berlin/Heidelberg, Germany, 2014; pp. 889–1010. ISBN 978-3-642-30138-4.

9. Seipke, R.F.; Kaltenpoth, M.; Hutchings, M.I. *Streptomyces* as Symbionts: An Emerging and Widespread Theme? *FEMS Microbiol. Rev.* **2012**, *36*, 862–876. [CrossRef]
10. Bérdy, J. Thoughts and Facts about Antibiotics: Where We Are Now and Where We Are Heading. *J. Antibiot.* **2012**, *65*, 385–395. [CrossRef]
11. Watve, M.G.; Tickoo, R.; Jog, M.M.; Bhole, B.D. How Many Antibiotics Are Produced by the Genus *Streptomyces*? *Arch. Microbiol.* **2001**, *176*, 386–390. [CrossRef]
12. Antoraz, S.; Santamaria, R.; Díaz, M.; Sanz, D.; Rodríguez, H. Towards a New Focus in Antibiotic and Drug Discovery from *Streptomyces Arsenal*. *Front. Microbiol.* **2015**, *6*, 461. [CrossRef]
13. Takahashi, Y.; Nakashima, T. Actinomycetes, an Inexhaustible Source of Naturally Occurring Antibiotics. *Antibiot.* **2018**, *7*, 45. [CrossRef]
14. Yao, L.; Liu, Q.; Wu, Z.M.; Li, K.T. Discovery and Evaluation on the Antibacterial and Cytotoxic Activities of a Novel Antifungalmycin N2 Produced from *Streptomyces* Sp. Strain N2. *Nat. Prod. Res.* **2019**, *35*, 2090–2094. [CrossRef] [PubMed]
15. Gohil, N.; Bhattacharjee, G.; Singh, V. *Chapter 1—An Introduction to Microbial Cell Factories for Production of Biomolecules*; Gohil, N., Bhattacharjee, G., Singh, V., Eds.; Academic Press: Cambridge, MA, USA, 2021; pp. 1–19. ISBN 978-0-12-821477-0.
16. Margalith, P.; Beretta, G. Rifomycin. XI. Taxonomic Study on *Streptomyces* Mediterranei Nov. Sp. *Mycopathol. Mycol. Appl.* **1960**, *13*, 321–330. [CrossRef]
17. Shapiro, S.; Vining, L.C. Nitrogen Metabolism and Chloramphenicol Production in *Streptomyces* Venezuelae. *Can. J. Microbiol.* **1983**, *29*, 1706–1714. [CrossRef] [PubMed]
18. Shih, H.D.; Liu, Y.C.; Hsu, F.L.; Mulabagal, V.; Dodda, R.; Huang, J.W. Fungichromin: A Substance from *Streptomyces Padanus* with Inhibitory Effects on Rhizoctonia Solani. *J. Agric. Food Chem.* **2003**, *51*, 95–99. [CrossRef] [PubMed]
19. Brautaset, T.; Sletta, H.; Degnes, K.F.; Sekurova, O.N.; Bakke, I.; Volokhan, O.; Andreassen, T.; Ellingsen, T.E.; Zotchev, S.B. New Nystatin-Related Antifungal Polyene Macrolides with Altered Polyol Region Generated via Biosynthetic Engineering of *Streptomyces Noursei*. *Appl. Environ. Microbiol.* **2011**, *77*, 6636–6643. [CrossRef] [PubMed]
20. Park, S.R.; Park, J.W.; Ban, Y.H.; Sohng, J.K.; Yoon, Y.J. 2-Deoxystreptamine-Containing Aminoglycoside Antibiotics: Recent Advances in the Characterization and Manipulation of Their Biosynthetic Pathways. *Nat. Prod. Rep.* **2013**, *30*, 11–20. [CrossRef] [PubMed]
21. Barreales, E.G.; Payero, T.D.; de Pedro, A.; Aparicio, J.F. Phosphate Effect on Filipin Production and Morphological Differentiation in *Streptomyces Filipinensis* and the Role of the PhoP Transcription Factor. *PLoS ONE* **2018**, *13*, e0208278. [CrossRef]
22. Ōmura, S.; Crump, A. The Life and Times of Ivermectin—A Success Story. *Nat. Rev. Microbiol.* **2004**, *2*, 984–989. [CrossRef]
23. Sadeghi, A.; Karimi, E.; Dahaji, P.A.; Javid, M.G.; Dalvand, Y.; Askari, H. Plant Growth Promoting Activity of an Auxin and Siderophore Producing Isolate of *Streptomyces* under Saline Soil Conditions. *World J. Microbiol. Biotechnol.* **2012**, *28*, 1503–1509. [CrossRef]
24. Armin, R.; Zühlke, S.; Grunewaldt-Stöcker, G.; Mahnkopp-Dirks, F.; Kusari, S. Production of Siderophores by an Apple Root-Associated *Streptomyces Ciscaucasicus* Strain GS2 Using Chemical and Biological OSMAC Approaches. *Molecules* **2021**, *26*, 3517. [CrossRef] [PubMed]
25. Nozari, R.M.; Ortolan, F.; Astarita, L.V.; Santarém, E.R. *Streptomyces* Spp. Enhance Vegetative Growth of Maize Plants under Saline Stress. *Braz. J. Microbiol.* **2021**, *52*, 1371–1383. [CrossRef] [PubMed]
26. El-Naggar, N.E.-A. Chapter 11—Streptomyces-Based Cell Factories for Production of Biomolecules and Bioactive Metabolites. In *Microbial Cell Factories Engineering for Production of Biomolecules*; Singh, V., Ed.; Academic Press: Cambridge, MA, USA, 2021; pp. 183–234. ISBN 978-0-12-821477-0.
27. Sanjivkumar, M.; Silambarasan, T.; Ananthi, S.; ThangaTharani, K. Biosynthesis and Characterization of Zinc Oxide Nanoparticles from an Estuarine-Associated Actinobacterium *Streptomyces* Spp. and Its Biotherapeutic Applications. *Arch. Microbiol.* **2021**, *204*, 17. [CrossRef]
28. Mechouche, M.S.; Merouane, F.; Messaad, C.E.H.; Golzadeh, N.; Vasseghian, Y.; Berkani, M. Biosynthesis, Characterization, and Evaluation of Antibacterial and Photocatalytic Methylene Blue Dye Degradation Activities of Silver Nanoparticles from *Streptomyces Tuirus* Strain. *Environ. Res.* **2022**, *204*, 112360. [CrossRef]
29. Khattab, A.; Babiker, E.; Saeed, H. *Streptomyces*: Isolation, Optimization of Culture Conditions and Extraction of Secondary Metabolites. *Int. Curr. Pharm. J.* **2016**, *5*, 27. [CrossRef]
30. Ding, W.; Tu, J.; Zhang, H.; Wei, X.; Ju, J.; Li, Q. Genome Mining and Metabolic Profiling Uncover Polycyclic Tetramate Macrolactams from *Streptomyces Koyangensis* SCSIO 5802. *Mar. Drugs* **2021**, *19*, 440. [CrossRef]
31. Duhsaki, L.; Mukherjee, S.; Rani, T.S.; Madhuprakash, J. Genome Analysis of *Streptomyces* Sp. UH6 Revealed the Presence of Potential Chitinolytic Machinery Crucial for Chitosan Production. *Environ. Microbiol. Rep.* **2022**, *14*, 431–442. [CrossRef] [PubMed]
32. Zhang, H.; Chen, Y.; Li, Y.; Song, Y.; Ma, J.; Ju, J. Secondary Metabolites and Biosynthetic Gene Clusters Analysis of Deep-Sea Hydrothermal Vent-Derived *Streptomyces* Sp. SCSIO ZS0520. *Mar. Drugs* **2022**, *20*, 393. [CrossRef] [PubMed]
33. Liu, T.; Ren, Z.; Chunyu, W.X.; Li, G.D.; Chen, X.; Zhang, Z.T.L.; Sun, H.B.; Wang, M.; Xie, T.P.; Wang, M.; et al. Exploration of Diverse Secondary Metabolites From *Streptomyces* Sp. YINM00001, Using Genome Mining and One Strain Many Compounds Approach. *Front. Microbiol.* **2022**, *13*, 831174. [CrossRef] [PubMed]
34. Rehan, M.; ALSohim, A.S.; Abidou, H.; Rasheed, Z.; Abdulmonem, W.A.L. Isolation, Identification, Biocontrol Activity, and Plant Growth Promoting Capability of a Superior *Streptomyces Tricolor* Strain HM10. *Pol. J. Microbiol.* **2021**, *70*, 245–256. [CrossRef]

35. Omar, A.F.; Abdelmageed, A.H.A.; Al-Turki, A.; Abdelhameid, N.M.; Sayyed, R.Z.; Rehan, M. Exploring the Plant Growth-Promotion of Four Streptomyces Strains from Rhizosphere Soil to Enhance Cucumber Growth and Yield. *Plants* **2022**, *11*, 3316. [CrossRef] [PubMed]
36. Page, A.L. Methods of Soil Analysis. In *Part 2—Chemical and Microbiological Properties*; The American Society of Agronomy, Inc.: Madison, WI, USA; Soil Science Society of America: Madison, WI, USA, 1982.
37. Rathje Jackson, M.L. Soil Chemical Analysis. Verlag: Prentice Hall, Inc., Englewood Cliffs, NJ. 1958, 498 S. DM 39.40. *Zeitschrift für Pflanzenernährung Düngung Bodenkd* **1959**, *85*, 251–252. [CrossRef]
38. Nelson, D.W.; Sommers, L.E. Total Carbon, Organic Carbon, and Organic Matter. In *Methods of Soil Analysis*; SSSA Book Series; American Society of Agronomy, Inc.: Madison, WI, USA; Soil Science Society of America, Inc.: Madison, WI, USA, 1996; pp. 961–1010. ISBN 9780891188667.
39. Gee, G.W.; Or, D. 2.4 Particle-Size Analysis. In *Methods of Soil Analysis*; SSSA Book Series; Soil Science Society of America, Inc.: Madison, WI, USA, 2002; pp. 255–293. ISBN 9780891188933.
40. Qureshi, K.A.; Bholay, A.D.; Rai, P.K.; Mohammed, H.A.; Khan, R.A.; Azam, F.; Jaremko, M.; Emwas, A.-H.; Stefanowicz, P.; Waliczek, M.; et al. Isolation, Characterization, Anti-MRSA Evaluation, and in-Silico Multi-Target Anti-Microbial Validations of Actinomycin X2 and Actinomycin D Produced by Novel *Streptomyces Smyrnaeus* UKAQ_23. *Sci. Rep.* **2021**, *11*, 14539. [CrossRef] [PubMed]
41. William, S.; Feil, H.; Copeland, A. Bacterial Genomic DNA Isolation Using CTAB. *Sigma* **2012**, *50*, 6876.
42. Kolmogorov, M.; Yuan, J.; Lin, Y.; Pevzner, P.A. Assembly of Long, Error-Prone Reads Using Repeat Graphs. *Nat. Biotechnol.* **2019**, *37*, 540–546. [CrossRef] [PubMed]
43. Vaser, R.; Sović, I.; Nagarajan, N.; Šikić, M. Fast and Accurate de Novo Genome Assembly from Long Uncorrected Reads. *Genome Res.* **2017**, *27*, 737–746. [CrossRef]
44. Oosterbroek, S.; Doorenspleet, K.; Nijland, R.; Jansen, L. Decona: From Demultiplexing to Consensus for Nanopore Amplicon Data. *ARPHA Conf. Abstr.* **2021**, *4*, e65029. [CrossRef]
45. Mikheenko, A.; Prjibelski, A.; Saveliev, V.; Antipov, D.; Gurevich, A. Versatile Genome Assembly Evaluation with QUAST-LG. *Bioinformatics* **2018**, *34*, i142–i150. [CrossRef]
46. Parks, D.H.; Imelfort, M.; Skennerton, C.T.; Hugenholtz, P.; Tyson, G.W. CheckM: Assessing the Quality of Microbial Genomes Recovered from Isolates, Single Cells, and Metagenomes. *Genome Res.* **2015**, *25*, 1043–1055. [CrossRef]
47. Tatusova, T.; DiCuccio, M.; Badretdin, A.; Chetvernin, V.; Nawrocki, E.P.; Zaslavsky, L.; Lomsadze, A.; Pruitt, K.D.; Borodovsky, M.; Ostell, J. NCBI Prokaryotic Genome Annotation Pipeline. *Nucleic Acids Res.* **2016**, *44*, 6614–6624. [CrossRef]
48. Meier-Kolthoff, J.P.; Göker, M. TYGS Is an Automated High-Throughput Platform for State-of-the-Art Genome-Based Taxonomy. *Nat. Commun.* **2019**, *10*, 2182. [CrossRef] [PubMed]
49. Ondov, B.D.; Treangen, T.J.; Melsted, P.; Mallonee, A.B.; Bergman, N.H.; Koren, S.; Phillippy, A.M. Mash: Fast Genome and Metagenome Distance Estimation Using MinHash. *Genome Biol.* **2016**, *17*, 132. [CrossRef] [PubMed]
50. Yoon, S.H.; Ha, S.; Lim, J.; Kwon, S.; Chun, J. A Large-Scale Evaluation of Algorithms to Calculate Average Nucleotide Identity. *Antonie Van Leeuwenhoek* **2017**, *110*, 1281–1286. [CrossRef] [PubMed]
51. Lagesen, K.; Hallin, P.; Rødland, E.A.; Staerfeldt, H.-H.; Rognes, T.; Ussery, D.W. RNAmmer: Consistent and Rapid Annotation of Ribosomal RNA Genes. *Nucleic Acids Res.* **2007**, *35*, 3100–3108. [CrossRef]
52. Camacho, C.; Coulouris, G.; Avagyan, V.; Ma, N.; Papadopoulos, J.; Bealer, K.; Madden, T.L. BLAST+: Architecture and Applications. *BMC Bioinform.* **2009**, *10*, 421. [CrossRef]
53. Blin, K.; Shaw, S.; Kloosterman, A.M.; Charlop-Powers, Z.; van Wezel, G.P.; Medema, M.H.; Weber, T. AntiSMASH 6.0: Improving Cluster Detection and Comparison Capabilities. *Nucleic Acids Res.* **2021**, *49*, W29–W35. [CrossRef]
54. Skinnider, M.A.; Johnston, C.W.; Gunabalasingam, M.; Merwin, N.J.; Kieliszek, A.M.; MacLellan, R.J.; Li, H.; Ranieri, M.R.M.; Webster, A.L.H.; Cao, M.P.T.; et al. Comprehensive Prediction of Secondary Metabolite Structure and Biological Activity from Microbial Genome Sequences. *Nat. Commun.* **2020**, *11*, 6058. [CrossRef]
55. Mistry, J.; Chuguransky, S.; Williams, L.; Qureshi, M.; Salazar, G.A.; Sonnhammer, E.L.L.; Tosatto, S.C.E.; Paladin, L.; Raj, S.; Richardson, L.J.; et al. Pfam: The Protein Families Database in 2021. *Nucleic Acids Res.* **2021**, *49*, D412–D419. [CrossRef]
56. Kautsar, S.A.; Blin, K.; Shaw, S.; Navarro-Muñoz, J.C.; Terlouw, B.R.; van der Hooft, J.J.J.; van Santen, J.A.; Tracanna, V.; Suarez Duran, H.G.; Pascal Andreu, V.; et al. MIBiG 2.0: A Repository for Biosynthetic Gene Clusters of Known Function. *Nucleic Acids Res.* **2020**, *48*, D454–D458. [CrossRef]
57. Lefort, V.; Desper, R.; Gascuel, O. FastME 2.0: A Comprehensive, Accurate, and Fast Distance-Based Phylogeny Inference Program. *Mol. Biol. Evol.* **2015**, *32*, 2798–2800. [CrossRef]
58. Farris, J.S. Estimating Phylogenetic Trees from Distance Matrices. *Am. Nat.* **1972**, *106*, 645–668. [CrossRef]
59. Zhao, B.; Lin, X.; Lei, L.; Lamb, D.C.; Kelly, S.L.; Waterman, M.R.; Cane, D.E. Biosynthesis of the Sesquiterpene Antibiotic Albaflavenone in *Streptomyces Coelicolor* A3(2). *J. Biol. Chem.* **2008**, *283*, 8183–8189. [CrossRef] [PubMed]
60. Bentley, S.D.; Chater, K.F.; Cerdeño-Tárraga, A.M.; Challis, G.L.; Thomson, N.R.; James, K.D.; Harris, D.E.; Quail, M.A.; Kieser, H.; Harper, D.; et al. Complete Genome Sequence of the Model Actinomycete *Streptomyces Coelicolor* A3(2). *Nature* **2002**, *417*, 141–147. [CrossRef] [PubMed]

61. Holmes, T.C.; May, A.E.; Zaleta-Rivera, K.; Ruby, J.G.; Skewes-Cox, P.; Fischbach, M.A.; DeRisi, J.L.; Iwatsuki, M.; Ōmura, S.; Khosla, C. Molecular Insights into the Biosynthesis of Guadinomine: A Type III Secretion System Inhibitor. *J. Am. Chem. Soc.* **2012**, *134*, 17797–17806. [CrossRef]
62. Zhang, W.; Wang, L.; Kong, L.; Wang, T.; Chu, Y.; Deng, Z.; You, D. Unveiling the Post-PKS Redox Tailoring Steps in Biosynthesis of the Type II Polyketide Antitumor Antibiotic Xantholipin. *Chem. Biol.* **2012**, *19*, 422–432. [CrossRef]
63. Xu, F.; Nazari, B.; Moon, K.; Bushin, L.B.; Seyedsayamdost, M.R. Discovery of a Cryptic Antifungal Compound from Streptomyces Albus J1074 Using High-Throughput Elicitor Screens. *J. Am. Chem. Soc.* **2017**, *139*, 9203–9212. [CrossRef]
64. Mohimani, H.; Kersten, R.D.; Liu, W.T.; Wang, M.; Purvine, S.O.; Wu, S.; Brewer, H.M.; Pasa-Tolic, L.; Bandeira, N.; Moore, B.S.; et al. Automated Genome Mining of Ribosomal Peptide Natural Products. *ACS Chem. Biol.* **2014**, *9*, 1545–1551. [CrossRef]
65. Pawlik, K.; Kotowska, M.; Chater, K.F.; Kuczek, K.; Takano, E. A Cryptic Type I Polyketide Synthase (Cpk) Gene Cluster in *Streptomyces Coelicolor* A3(2). *Arch. Microbiol.* **2007**, *187*, 87–99. [CrossRef]
66. O'Rourke, S.; Wietzorrek, A.; Fowler, K.; Corre, C.; Challis, G.L.; Chater, K.F. Extracellular Signalling, Translational Control, Two Repressors and an Activator All Contribute to the Regulation of Methylenomycin Production in *Streptomyces Coelicolor*. *Mol. Microbiol.* **2009**, *71*, 763–778. [CrossRef]
67. Metsä-Ketelä, M.; Palmu, K.; Kunnari, T.; Ylihonko, K.; Mäntsälä, P. Engineering Anthracycline Biosynthesis toward Angucyclines. *Antimicrob. Agents Chemother.* **2003**, *47*, 1291–1296. [CrossRef]
68. Palmu, K.; Ishida, K.; Mäntsälä, P.; Hertweck, C.; Metsä-Ketelä, M. Artificial Reconstruction of Two Cryptic Angucycline Antibiotic Biosynthetic Pathways. *ChemBioChem* **2007**, *8*, 1577–1584. [CrossRef] [PubMed]
69. Kersten, R.D.; Yang, Y.-L.; Xu, Y.; Cimermancic, P.; Nam, S.-J.; Fenical, W.; Fischbach, M.A.; Moore, B.S.; Dorrestein, P.C. A Mass Spectrometry-Guided Genome Mining Approach for Natural Product Peptidogenomics. *Nat. Chem. Biol.* **2011**, *7*, 794–802. [CrossRef]
70. Fagerholm, A.E.; Habrant, D.; Koskinen, A.M.P. Calyculins and Related Marine Natural Products as Serine-Threonine Protein Phosphatase PP1 and PP2A Inhibitors and Total Syntheses of Calyculin A, B, and C. *Mar. Drugs* **2010**, *8*, 122–172. [CrossRef] [PubMed]
71. Wakimoto, T.; Egami, Y.; Nakashima, Y.; Wakimoto, Y.; Mori, T.; Awakawa, T.; Ito, T.; Kenmoku, H.; Asakawa, Y.; Piel, J.; et al. Calyculin Biogenesis from a Pyrophosphate Protoxin Produced by a Sponge Symbiont. *Nat. Chem. Biol.* **2014**, *10*, 648–655. [CrossRef] [PubMed]
72. Pfennig, F.; Schauwecker, F.; Keller, U. Molecular Characterization of the Genes of Actinomycin Synthetase I and of a 4-Methyl-3-Hydroxyanthranilic Acid Carrier Protein Involved in the Assembly of the Acylpeptide Chain of Actinomycin in *Streptomyces*. *J. Biol. Chem.* **1999**, *274*, 12508–12516. [CrossRef]
73. Keller, U.; Lang, M.; Crnovcic, I.; Pfennig, F.; Schauwecker, F. The Actinomycin Biosynthetic Gene Cluster of *Streptomyces Chrysomallus*: A Genetic Hall of Mirrors for Synthesis of a Molecule with Mirror Symmetry. *J. Bacteriol.* **2010**, *192*, 2583–2595. [CrossRef]
74. Schauwecker, F.; Pfennig, F.; Grammel, N.; Keller, U. Construction and in Vitro Analysis of a New Bi-Modular Polypeptide Synthetase for Synthesis of N-Methylated Acyl Peptides. *Chem. Biol.* **2000**, *7*, 287–297. [CrossRef]
75. Xiao, C.; Xu, C.; Zhang, J.; Jiang, W.; Zhang, X.; Yang, C.; Xu, J.; Zhang, Y.; Zhou, T. Soil Microbial Communities Affect the Growth and Secondary Metabolite Accumulation in Bletilla Striata (Thunb.) Rchb. F. *Front. Microbiol.* **2022**, *13*, 916418. [CrossRef]
76. Zhao, Q.; Wang, L.; Luo, Y. Recent Advances in Natural Products Exploitation in *Streptomyces* via Synthetic Biology. *Eng. Life Sci.* **2019**, *19*, 452–462. [CrossRef]
77. Liu, R.; Deng, Z.; Liu, T. *Streptomyces* Species: Ideal Chassis for Natural Product Discovery and Overproduction. *Metab. Eng.* **2018**, *50*, 74–84. [CrossRef]
78. Sarmiento-Vizcaíno, A.; Martín, J.; Reyes, F.; García, L.A.; Blanco, G. Bioactive Natural Products in Actinobacteria Isolated in Rainwater From Storm Clouds Transported by Western Winds in Spain. *Front. Microbiol.* **2021**, *12*, 773095. [CrossRef] [PubMed]
79. Yang, Z.; He, J.; Wei, X.; Ju, J.; Ma, J. Exploration and Genome Mining of Natural Products from Marine *Streptomyces*. *Appl. Microbiol. Biotechnol.* **2020**, *104*, 67–76. [CrossRef] [PubMed]
80. Paulus, C.; Rebets, Y.; Tokovenko, B.; Nadmid, S.; Terekhova, L.P.; Myronovskyi, M.; Zotchev, S.B.; Rückert, C.; Braig, S.; Zahler, S.; et al. New Natural Products Identified by Combined Genomics-Metabolomics Profiling of Marine *Streptomyces* Sp. MP131-18. *Sci. Rep.* **2017**, *7*, 42382. [CrossRef]
81. Lee, N.; Kim, W.; Hwang, S.; Lee, Y.; Cho, S.; Palsson, B.; Cho, B.-K. Thirty Complete *Streptomyces* Genome Sequences for Mining Novel Secondary Metabolite Biosynthetic Gene Clusters. *Sci. Data* **2020**, *7*, 55. [CrossRef]
82. Jaroszewicz, W.; Bielańska, P.; Lubomska, D.; Kosznik-Kwaśnicka, K.; Golec, P.; Grabowski, Ł.; Wieczerzak, E.; Dróżdż, W.; Gaffke, L.; Pierzynowska, K.; et al. Antibacterial, Antifungal and Anticancer Activities of Compounds Produced by Newly Isolated *Streptomyces* Strains from the Szczelina Chochołowska Cave (Tatra Mountains, Poland). *Antibiotics* **2021**, *10*, 1212. [CrossRef]
83. Santos-Beneit, F.; Ceniceros, A.; Nikolaou, A.; Salas, J.A.; Gutierrez-Merino, J. Identification of Antimicrobial Compounds in Two *Streptomyces* Sp. Strains Isolated from Beehives. *Front. Microbiol.* **2022**, *13*, 742168. [CrossRef] [PubMed]
84. Kim, Y.J.; Kim, J.; Rho, J.-Y. Antifungal Activities of *Streptomyces Blastmyceticus* Strain 12-6 Against Plant Pathogenic Fungi. *Mycobiology* **2019**, *47*, 329–334. [CrossRef]
85. Le, K.D.; Yu, N.H.; Park, A.R.; Park, D.-J.; Kim, C.-J.; Kim, J.-C. *Streptomyces* sp. AN090126 as a Biocontrol Agent against Bacterial and Fungal Plant Diseases. *Microorganisms* **2022**, *10*, 791. [CrossRef]

86. Tomaseto, A.A.; Alpiste, M.C.; de Castro Nassar, A.F.; Destéfano, S.A.L. Antibacterial activity of phytopathogenic *Streptomyces* strains against bacteria associated to clinical diseases. *Arq. Inst. Biol.* **2020**, *87*, e0142020. [CrossRef]
87. Shah, M.; Gul, S.; Amjad, A.; Javed, M.S.; Fatima, B.; Nawaz, H.; Ishaq, J. Genome Mining of *Streptomyces Formicae* KY5 for Potential Drug like Natural Products Characterizations. *J. Proteomics Bioinform.* **2019**, *12*, 122–127. [CrossRef]
88. Komaki, H.; Ishikawa, A.; Ichikawa, N.; Hosoyama, A.; Hamada, M.; Harunari, E.; Nihira, T.; Panbangred, W.; Igarashi, Y. Draft Genome Sequence of *Streptomyces* Sp. MWW064 for Elucidating the Rakicidin Biosynthetic Pathway. *Stand. Genom. Sci.* **2016**, *11*, 83. [CrossRef] [PubMed]
89. Moser, S.; Pichler, H. Identifying and Engineering the Ideal Microbial Terpenoid Production Host. *Appl. Microbiol. Biotechnol.* **2019**, *103*, 5501–5516. [CrossRef] [PubMed]
90. Peralta-Yahya, P.P.; Ouellet, M.; Chan, R.; Mukhopadhyay, A.; Keasling, J.D.; Lee, T.S. Identification and Microbial Production of a Terpene-Based Advanced Biofuel. *Nat. Commun.* **2011**, *2*, 483. [CrossRef] [PubMed]
91. Zhang, H.; Liu, Q.; Cao, Y.; Feng, X.; Zheng, Y.; Zou, H.; Liu, H.; Yang, J.; Xian, M. Microbial Production of Sabinene—A New Terpene-Based Precursor of Advanced Biofuel. *Microb. Cell Fact.* **2014**, *13*, 20. [CrossRef] [PubMed]
92. Phelan, R.M.; Sekurova, O.N.; Keasling, J.D.; Zotchev, S.B. Engineering Terpene Biosynthesis in *Streptomyces* for Production of the Advanced Biofuel Precursor Bisabolene. *ACS Synth. Biol.* **2015**, *4*, 393–399. [CrossRef]
93. Oldfield, E.; Lin, F.Y. Terpene Biosynthesis: Modularity Rules. *Angew. Chem. Int. Ed. Engl.* **2012**, *51*, 1124–1137. [CrossRef]
94. Yamada, Y.; Kuzuyama, T.; Komatsu, M.; Shin-ya, K.; Omura, S.; Cane, D.E.; Ikeda, H. Terpene Synthases Are Widely Distributed in Bacteria. *Proc. Natl. Acad. Sci. USA* **2015**, *112*, 857–862. [CrossRef]
95. Wenski, S.L.; Thiengmag, S.; Helfrich, E.J.N. Complex Peptide Natural Products: Biosynthetic Principles, Challenges and Opportunities for Pathway Engineering. *Synth. Syst. Biotechnol.* **2022**, *7*, 631–647. [CrossRef]
96. Minowa, Y.; Araki, M.; Kanehisa, M. Comprehensive Analysis of Distinctive Polyketide and Nonribosomal Peptide Structural Motifs Encoded in Microbial Genomes. *J. Mol. Biol.* **2007**, *368*, 1500–1517. [CrossRef]
97. Silakowski, B.; Kunze, B.; Müller, R. Multiple Hybrid Polyketide Synthase/Non-Ribosomal Peptide Synthetase Gene Clusters in the Myxobacterium Stigmatella Aurantiaca. *Gene* **2001**, *275*, 233–240. [CrossRef]
98. Minami, A.; Ugai, T.; Ozaki, T.; Oikawa, H. Predicting the Chemical Space of Fungal Polyketides by Phylogeny-Based Bioinformatics Analysis of Polyketide Synthase-Nonribosomal Peptide Synthetase and Its Modification Enzymes. *Sci. Rep.* **2020**, *10*, 13556. [CrossRef] [PubMed]
99. Hwang, S.; Lee, N.; Cho, S.; Palsson, B.; Cho, B.-K. Repurposing Modular Polyketide Synthases and Non-Ribosomal Peptide Synthetases for Novel Chemical Biosynthesis. *Front. Mol. Biosci.* **2020**, *7*, 87. [CrossRef] [PubMed]
100. Wei, Y.; Zhang, L.; Zhou, Z.; Yan, X. Diversity of Gene Clusters for Polyketide and Nonribosomal Peptide Biosynthesis Revealed by Metagenomic Analysis of the Yellow Sea Sediment. *Front. Microbiol.* **2018**, *9*, 295. [CrossRef] [PubMed]
101. Letzel, A.-C.; Pidot, S.J.; Hertweck, C. Genome Mining for Ribosomally Synthesized and Post-Translationally Modified Peptides (RiPPs) in Anaerobic Bacteria. *BMC Genom.* **2014**, *15*, 983. [CrossRef]
102. Komaki, H.; Tamura, T. Polyketide Synthase and Nonribosomal Peptide Synthetase Gene Clusters in Type Strains of the Genus Phytohabitans. *Life* **2020**, *10*, 257. [CrossRef]
103. Zheng, Y.; Saitou, A.; Wang, C.-M.; Toyoda, A.; Minakuchi, Y.; Sekiguchi, Y.; Ueda, K.; Takano, H.; Sakai, Y.; Abe, K.; et al. Genome Features and Secondary Metabolites Biosynthetic Potential of the Class Ktedonobacteria. *Front. Microbiol.* **2019**, *10*, 893. [CrossRef]